Self-Assembly of a Quinobenzoxazine-Mg^{2+} Complex on DNA: A New Paradigm for the Structure of a Drug-DNA Complex and Implications for the Structure of the Quinolone Bacterial Gyrase-DNA Complex

Jun-Yao Fan, Daekyu Sun, Hongtao Yu, Sean M. Kerwin,* and Laurence H. Hurley*

Division of Medicinal Chemistry, College of Pharmacy, The University of Texas at Austin, Austin, Texas 78712-1074

Received November 16, 1994[⊗]

The quinobenzoxazine compounds A-62176 and A-85226 belong to a novel class of antineoplastic agents that are catalytic inhibitors of topoisomerase II and also structural analogs of the antibacterial DNA gyrase inhibitor Norfloxacin. *In vitro* studies have shown that their antineoplastic activity is dependent upon the presence of divalent metal ions such as Mg^{2+} and Mn^{2+}, although the precise role of these ions in the mechanism of action is unknown. In this study we have investigated the structures of the binary complex between the quinobenzoxazines and Mg^{2+} and the ternary complex between quinobenzoxazine-Mg^{2+} and DNA. The stoichiometry of the binary and ternary complexes and the biophysical studies suggest that a 2:2 drug:Mg^{2+} complex forms a "heterodimer complex" with respect to DNA in which one drug molecule is intercalated into DNA and the second drug molecule is externally bound, held to the first molecule by two Mg^{2+} bridges, which themselves are chelated to phosphates on DNA. There is a cooperativity in binding of the quinobenzoxazines to DNA, and a 4:4 drug:Mg^{2+} complex is proposed in which the two externally bound molecules from two different 2:2 dimers interact via $\pi-\pi$ interactions. The externally bound quinobenzoxazine molecules can be replaced by the quinolone antibacterial compound Norfloxacin to form mixed-structure dimers on DNA. Based upon the proposed model for the 2:2 quinobenzoxazine:Mg^{2+} complex on DNA, a parallel model for the antibacterial quinolone-Mg^{2+}-DNA gyrase complex is proposed that relies upon the ATP-fueled unwinding of DNA by gyrase downstream of the cleavable complex site. These models, which have analogies to leucine zippers, represent a new paradigm for the structure of drug-DNA complexes. In addition, these models have important implications for the design of new gyrase and topoisomerase II inhibitors, in that optimization for structure-activity relationships should be carried out on two different quinolone molecules rather than a single molecule.

Introduction

Research at Abbott Laboratories with the objective to discover novel anticancer drugs has resulted in the identification of a number of synthetic quinolone analogs with excellent *in vivo* antineoplastic activity.[1,2] This biological activity differs from that of the parent quinolones, typified by Norfloxacin, which show antibacterial activity but are devoid of antineoplastic activity. The quinobenzoxazine compounds A-62176 (1-(3-aminopyrrolidin-1-yl)-2-fluoro-4-oxo-4*H*-quino[2,3,4-*ij*][1,4]benzoxazine-5-carboxylic acid) and A-85226 (3-amino-1-(3-aminopyrrolidin-1-yl)-2-fluoro-4-oxo-4*H*-quino[2,3,4-*ij*][1,4]benzoxazine-5-carboxylic acid) (Figure 1) are two examples of these agents and have been identified as part of a novel class of synthetic antineoplastic agents.[2] While the quinobenzoxazines are structurally related to the quinolone bacterial gyrase inhibitor Norfloxacin, they possess a planar tetracyclic ring structure in place of the fused bicyclic ring system of Norfloxacin (Figure 1). Recent studies at Abbott Laboratories demonstrate that the quinobenzoxazine compounds are active against a wide range of human and murine cell lines *in vitro*, have curative activity against systemic tumors in mice, and have reproducible cytotoxic activity in a number of solid tumor models (Shen, unpublished results).[2] The molecular basis for the anticancer activity of the quinobenzoxazines is not understood but is believed to be mediated by their interaction with topoisomerase II. Recently, Permana and co-workers have shown that the quinobenzoxazines are potent mammalian DNA topoisomerase II inhibitors but do not cause topoisomerase II-mediated strand breaks.[3] Thus, it has been proposed that these compounds inhibit the DNA topoisomerase II reaction at a step *prior* to the formation of the "cleavage complex" intermediate. The DNA binding

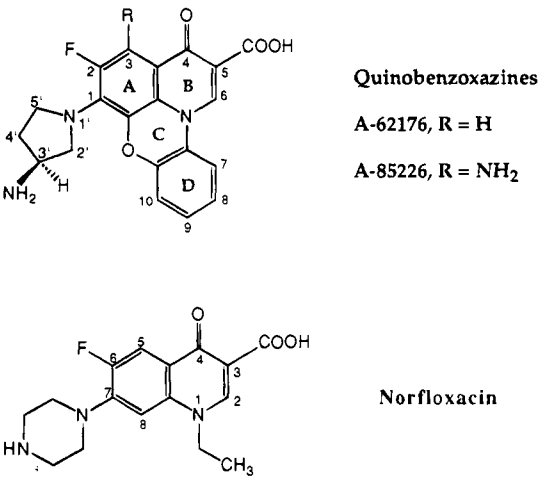

Figure 1. Structures of the quinobenzoxazine (A-62176 and A-85226) and quinolone (Norfloxacin) compounds used in this study. In the case of the quinobenzoxazines, the *S* enantiomers were used.

* Address correspondence to either of these authors. Telephone: (512) 471-4842. FAX: (512) 471-2746.

[⊗] Abstract published in *Advance ACS Abstracts*, January 15, 1995.

0022-2623/95/1838-0408$09.00/0

affinity of various quinobenzoxazines to DNA parallels their cytotoxic potency.[4] However, the mode of interaction (e.g., intercalation vs groove binding) of the quinobenzoxazines with DNA was undefined. While many studies on the mechanism of action of the parent quinolones have been reported, there are conflicting reports, particularly in regard to the role played by DNA in the mechanism of action of the quinolones.[5–8] A large amount of biological data has suggested that DNA gyrase is the intracellular target for quinolones.[6,7,9–12] However, several recent reports have shown that the quinolones do not bind to DNA gyrase but instead bind to DNA.[8,13–16] The Abbott investigators have proposed a novel cooperative quinolone–DNA binding model and suggested that self-associated Norfloxacin molecules bind via hydrogen bonds to transient single-stranded regions in DNA that are produced by gyrase during the intermediate gate-opening step of the duplex DNA supercoiling process.[15] Significantly, Norfloxacin is also able to unwind DNA but only in the presence of Mg^{2+} ions.[17,18] Drug-induced DNA unwinding, which is measured in an assay using closed circular DNA, has been considered in many cases as indicative of intercalative binding by drugs to DNA. However, the DNA unwinding efficiency of Norfloxacin is far less than that for adriamycin and daunomycin, which are known to intercalate into duplex DNA.[17] In fact, the putative unwinding angle for Norfloxacin is less than 11°, which is the minimum possible unwinding angle consistent with intercalation.[19] Also, the instability to electrophoresis of the DNA–Norfloxacin complex is only consistent with either weak intercalative binding by Norfloxacin in native duplex DNA or dissociative release of the ligand during the assay.[17,18]

Like Norfloxacin, preliminary mechanism of action studies have shown that DNA binding of the quinobenzoxazines is dependent upon the presence of divalent metal ions (Shen, unpublished results). However, the role of these divalent ions in the binding of the quinobenzoxazines to DNA is unknown. To account for the Mg^{2+} dependency of Norfloxacin binding to DNA, the lack of evidence for intercalation, and the preference for binding to single-stranded DNA, Palumbo and co-workers have proposed a new model for DNA binding in which Mg^{2+} acts as a bridge between the phosphate groups of the nucleic acid and the carbonyl and carboxyl groups of Norfloxacin, although direct experimental evidence is lacking.[5,18] Stacking interactions between the Norfloxacin aromatic rings and the DNA bases in single-stranded regions have been proposed to further stabilize the ternary (Norfloxacin–Mg^{2+}–DNA) complex.[5,18] The present study of the quinobenzoxazines demonstrates that for these analogs of the antibacterial quinolones *both* duplex DNA unwinding and a noncovalent binding mode to DNA are Mg^{2+} dependent. However, moderate structural differences between quinolone and quinobenzoxazine compounds result in large differences in their biological activities, as the former are antibacterial agents and the latter are antineoplastic agents. Our results with the quinobenzoxazine antineoplastics provide firm experimental evidence for the proposed binding role of Mg^{2+} in the complex with DNA[5] and suggest an alternative mechanism for interaction of the antibacterial compounds with the partially unwound *duplex* DNA produced by the interaction with topoisomerase.

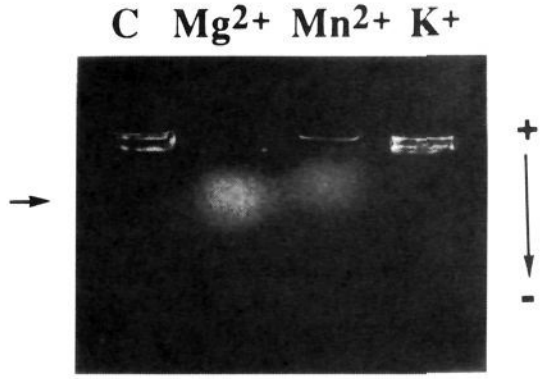

Figure 2. Fluorescence-detected gel electrophoresis of A-62176 in the absence (C) and presence of Mg^{2+}, Mn^{2+}, or K^+ ion. Each lane contains 2 μL of a 10 mM solution of A-62176 containing Mg^{2+}, Mn^{2+}, and K^+, respectively, at a drug:metal ion ratio of 1:50. The arrow points to the A-62176–Mg^{2+} or A-62176–Mn^{2+} complex.

In this article, the binary complex between the quinobenzoxazines and Mg^{2+} and the ternary complex between quinobenzoxazine, Mg^{2+}, and DNA have been investigated using a variety of experimental methods, including ^{1}H- and ^{31}P-NMR, FT-IR, UV–vis spectroscopy, viscometry, and gel electrophoresis, in an attempt to gain insight into the binding specificity, ligand-induced conformational transitions in DNA, cooperativity in binding, and drug binding modes to DNA. A-85226, an amino analog of A-62176 (Figure 1), was used in the FT-IR, NMR, and viscometry studies because it has greater solubility than A-62176 in water. Last, the combined interactions of a quinobenzoxazine, ethidium bromide, or echinomycin together with Norfloxacin and DNA in the presence of Mg^{2+} have been studied to attempt to explain the different biological activities of the quinolone and quinobenzoxazine compounds. Some of this work has been published in preliminary form.[4,20,21]

Results

1. The Structure and Stoichiometry of the Coordination Complex Formed between the Quinobenzoxazines and Divalent Metal Ions. Fluorescence Detection of Quinobenzoxazine–Metal Ion Complexes That Migrate during Agarose Gel Electrophoresis. The ability of A-62176 to form cationic complexes with divalent metal ions was probed using agarose gel electrophoresis (Figure 2). Aliquots (2 μL) of a 4 mM aqueous solution of A-62176, containing either Mg^{2+}, Mn^{2+}, or K^+ (all at a 1:50 drug:metal ion ratio), were loaded onto a 2.5% agarose gel and subjected to electrophoresis at pH 8.0. The intrinsic fluorescence of A-62176, upon irradiation with UV light, was exploited to detect the location of A-62176 and its complexes in the gel. The lanes having a combination of A-62176 with Mg^{2+} or Mn^{2+} show formation of a stable complex (see arrow in Figure 2), which migrates into the gel toward the cathode. In contrast, the sample of A-62176 in the presence of K^+ or in the absence of metal ions did not migrate into the gel. In the absence of metal ions, A-62176 is zwitterionic at pH 8; therefore, it does not migrate to the cathode. In the presence of Mg^{2+} and Mn^{2+}, the migration of the drug complex indicates that a positively charged complex is formed. The fact that the drug does not migrate in the presence

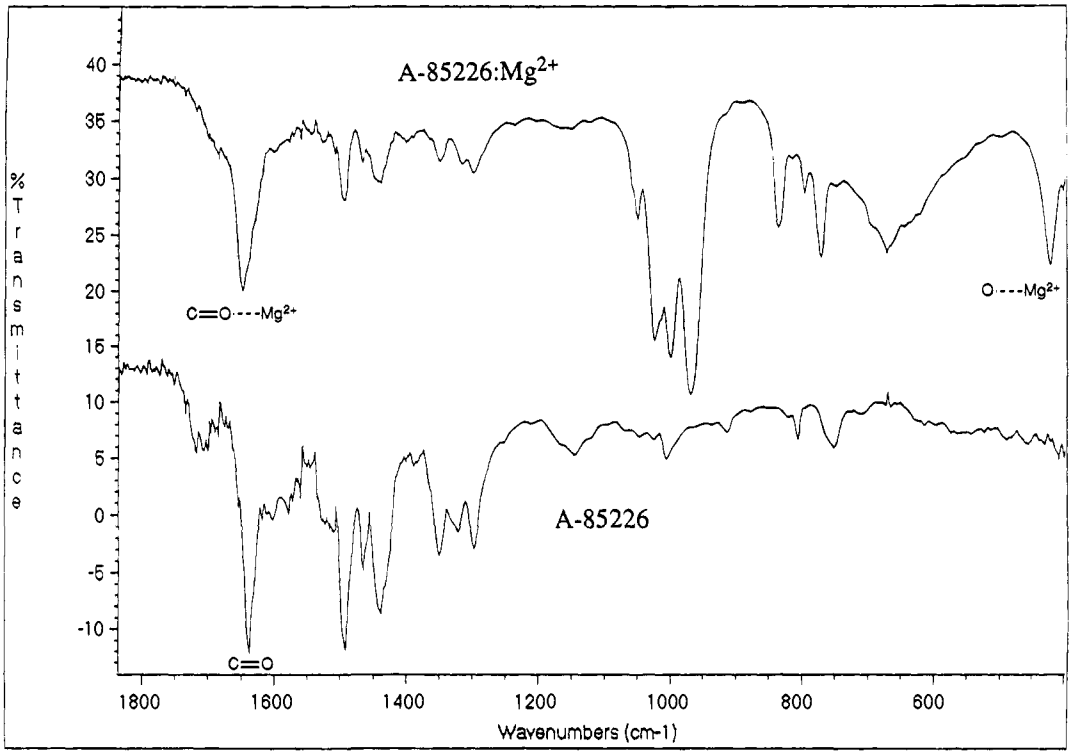

Figure 3. Partial FT-IR spectra in the range 1825–400 cm^{-1} of A-85226 (lower scan) and the A-85226–Mg^{2+} complex (upper scan), both taken in a KBr disk. The units on the y axis refer only to the upper spectrum; the lower spectrum has been scaled and displaced relative to the upper spectrum to aid in comparison.

of K^+ indicates there is no complex formation with univalent metal ions.

In a second experiment, aliquots of the A-62176–Mg^{2+} mixture within a range of drug:Mg^{2+} ratios (1:0.5–1:100) were applied to a 2.5% agarose gel (data not shown). Very little of the A-62176–Mg^{2+} complex migrated into the gel in mixtures having drug:Mg^{2+} ratios of less than 1:50. Since complex formation is only seen when the ratio of A-62176:Mg^{2+} is at least 1:50, this suggests that the complex is relatively unstable and that a large excess of Mg^{2+} is needed in order to drive the complex formation between drug and Mg^{2+} to completion.

Characterization of the Quinobenzoxazine–Mg^{2+} Complex by IR. Infrared spectral analysis has been used previously to study the complexes formed between quinolones and magnesium, as well as other divalent metal ions.[22] We sought to extend these studies to the quinobenzoxazine–Mg^{2+} complexes. For these experiments, we employed the quinobenzoxazine A-85226 because of its relatively higher solubility.

The IR spectra of the A-85226–Mg^{2+} and the A-85226–Mg^{2+} complexes in KBr disks are shown in Figure 3. In the lower spectrum, the ketonic group for free A-85226 has a strong IR band at 1640 cm^{-1}, typical of the ketonic group in 1,4-dihydro-4-oxoquinolines.[23] The carbonyl of the carboxylic acid of the free drug has a weaker band at 1700 cm^{-1}. In the A-85226–Mg^{2+} complex, the corresponding IR bands are weaker (upper spectrum, Figure 3). The band for the carboxylate carbonyl clearly shifts to a lower frequency (1685 cm^{-1}). However, due to interference by other bands in the same region, it is not clear that the ketonic band also shifts. A typical Mg^{2+}–O asymmetrical stretching frequency[24] at 426 cm^{-1} is also seen for the complex. A parallel experiment for the Norfloxacin–Mg^{2+} complex also shows the same change for the carboxylate carbonyl/ketonic bands and the formation of a new Mg^{2+}–O stretching frequency at 423 cm^{-1} (data not shown).

Job Titration Analysis of the A-62176–Mn^{2+} Complex. Job titration analysis[25,26] was used to determine the stoichiometry of metal–ligand complexes. Our agarose gel electrophoresis experiments indicated that A-62176 forms complexes with both magnesium and manganese but that the relative instability of the magnesium complex dictates the use of excess magnesium to drive complex formation to completion. Therefore, we used Mn^{2+} in this experiment. Absorbance titration of A-62176 by $MnCl_2$ was performed in MeOH. Upon addition of $MnCl_2$, the intensity of both absorption bands at 320 and 395 nm increased, but both bands shifted in opposite directions (Figure 4A); i.e., while the 320 nm band shifted to the blue, the 395 nm band shifted to the red. Up to a 1:1 ratio of A-62176:Mn^{2+}, there were two isobestic points at 326 and 370 nm, indicative of complex formation. However, further addition of Mn^{2+} caused the isobestic points to shift. We interpret this to mean that a new type of metal–drug complex is forming. The Job titration analysis for A-62176 with Mn^{2+} was performed at 320 nm in MeOH at room temperature. The mole fraction of Mn^{2+} was varied between 0 and 1. The normalized plot in Figure 4B shows a distinctive maximum at $x_{drug} = 0.50$ (mole fraction of drug), indicating that the stoichiometry of the drug–Mn^{2+} complex is 1:1, 2:2, etc.

2. The Quinobenzoxazines Bind to DNA, and the Binding to DNA Is Dependent upon Divalent Cations. DNase I Footprinting Analysis. A typical DNase I digestion pattern for the 63-bp oligomer (oligomer 1 in the Experimental Section) complexed with various concentrations of A-62176 in the presence of $MgCl_2$ (2 mM) is shown in Figure 5, left. The densito-

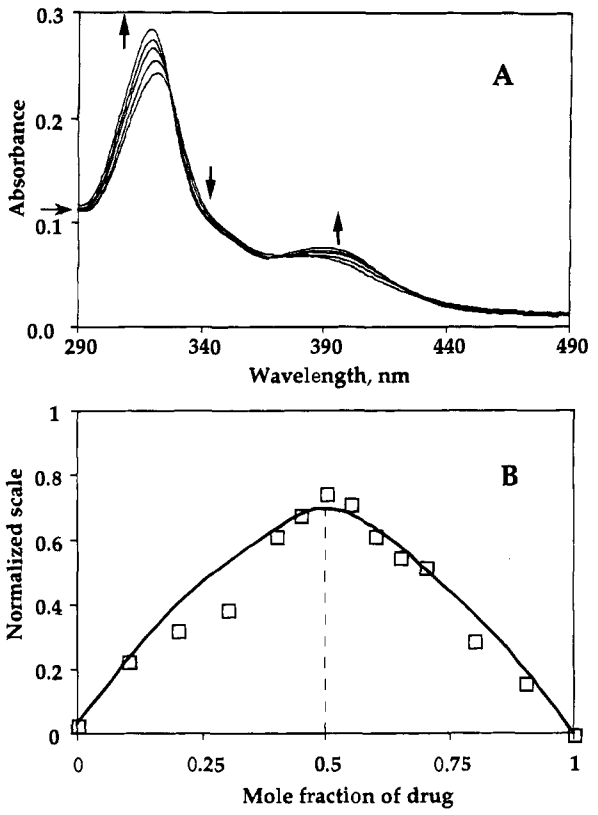

Figure 4. (A) UV–vis titration of a 30 μM methanolic solution of A-62176 with Mn^{2+} at room temperature. Plots from bottom to top in respect to the absorption at 320 nm are molar ratios of $[Mn^{2+}]/[A\text{-}62176] = 0$, 0.2, 0.4, 0.6, and 0.9. The arrow on the y axis indicates the spectrum of the drug in the absence of Mn^{2+}. (B) Job titration plot[25] for the A-62176–Mn^{2+} complex in methanol at room temperature. The total concentration of drug and Mn^{2+} is 100 μM.

metric scans in Figure 5, right, correspond to lanes 1–4 of the left panel. At the lowest concentration of A-62176 (lane 2), it is clear that A-62176 first interacts with the GC-rich region of oligomer 1 (brackets A–D in the left panel and scans corresponding to lanes 1 and 2 in the right panel). However, at the two lowest concentrations of A-62176 (lanes 2 and 3), the central region of the 63-bp oligomer (bracket E) that contains the T_7-tract shows *enhanced* DNase I cleavage in the presence of A-62176. One interpretation of this observation is that the presumed local unwinding of the T-tract due to the binding of A-62176 to the adjacent GC-rich region then renders this normally insensitive AT region susceptible to DNase I cleavage. In the presence of increasing drug concentrations (lanes 3–5), all regions of the DNA oligomer show diminished cleavage, except for the T-tract region, which only shows diminished cleavage in the presence of the highest concentration of A-62176. These results suggest that the interaction between A-62176 and DNA may involve a cooperative binding mechanism in which the binding of A-62176 to the GC-rich regions of the oligomer facilitates the subsequent binding of A-62176 at adjacent AT-rich regions.

The ability of A-62176 to bind to DNA is dependent upon the concentration of Mg^{2+}, as shown in Figure 6. Inspection of the autoradiograph (Figure 6) reveals that the DNase I cleavage pattern of the drug–DNA complex in the absence of Mg^{2+} (lane 2) is only slightly different from the cleavage pattern in the absence of any ligand (lane 1). However, increasing the Mg^{2+} concentration in the presence of a constant amount of A-62176 results in increased protection from DNase I cleavage (see brackets A–C). The DNA binding sites do not become saturated until the concentration of Mg^{2+} reaches 1 mM. Therefore, this DNase I footprinting result shows that the cooperative binding of A-62176 to DNA, which results in inhibition of DNase I cleavage, is dependent upon Mg^{2+} concentration.

Spectrophotometric Analysis. The binding of A-62176 to calf thymus DNA in the absence and presence of Mg^{2+} was also measured spectrophotometrically, and the results are shown in Figure 7. The free quinobenzoxazines show absorption peaks at 320 and 380 nm. Incremental addition of calf thymus DNA to drug solution in the absence of Mg^{2+} causes a slight blue shift and a decrease in absorbance only at the 320 nm peak of A-62176 (Figure 7A). In contrast, a red shift and reduction in absorption in both the 320 and 380 nm peaks, as well as three clear isobestic points (at 328, 345, and 414 nm), are observed when a solution of A-62176 containing 10 mM $MgCl_2$ is titrated with the DNA stock solution. Figure 7C shows the absorption change of A-62176 at 380 nm upon addition of DNA in the presence and absence of Mg^{2+}. While very little change in the absorption is observed in the absence of Mg^{2+}, a significant decrease in absorption is observed in the presence of Mg^{2+}. Since A-85226 behaves in a similar manner, the 380 nm absorption peak of the quinobenzoxazines can be used to monitor the divalent metal ion-specific binding of these drugs to DNA.

3. The Quinobenzoxazine Antineoplastic Agents Form Ternary Complexes with DNA in which Mg^{2+} Bridges between the Intercalated Drug and a Phosphate Oxygen in DNA. The Quinobenzoxazines Form Intercalation Complexes with DNA in the Presence of Mg^{2+} Ions. (i) Topoisomerase Relaxation Assay. The topoisomerase I-induced relaxation assay was carried out using supercoiled DNA, as described previously,[27] to test the helix unwinding ability of A-62176. Supercoiled DNA was incubated in the presence of magnesium and increasing concentrations of A-62176, then the DNA–drug complexes were incubated with topoisomerase I, and the resulting DNA topoisomers were separated by agarose gel electrophoresis. In the absence of added drug, a single band corresponding to relaxed circular DNA is produced; however, in the presence of increasing concentrations of A-62176, well-defined bands representing different topological forms, which migrate faster than the relaxed form, are produced (Sun and Hurley, data not shown). This result provides excellent evidence for an intercalation mechanism for A-62176 binding to DNA but in itself does not rule out minor groove binding with concomitant unwinding.

(ii) Viscometry Measurements. Viscometry measurements were used to further explore the binding mechanism of the quinobenzoxazines to DNA. In these experiments, the effect of A-85226, either in the presence or absence of Mg^{2+}, on the viscosity of sonicated calf thymus DNA was examined (Figure 8). For comparison, the viscometric titration profile of the contour length ratio of DNA (L/L_0) against moles of drug added per mole of DNA base pair (ν) for ethidium bromide, a classic intercalator, is also shown in Figure 8.

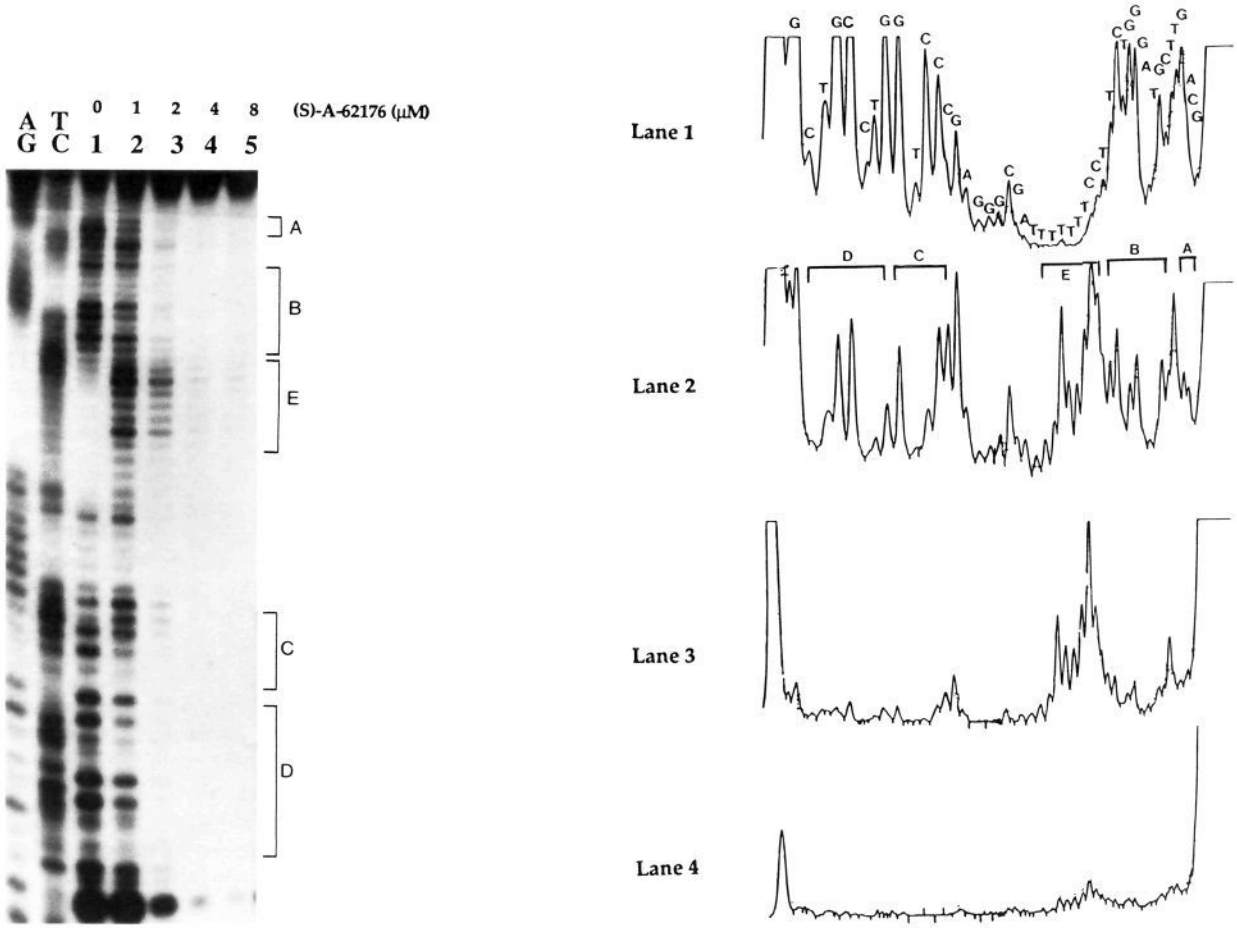

Figure 5. (Left) DNase I footprinting of oligomer 1 (for sequence, see Experimental Section) in the absence (lane 1) or presence (lanes 2−5) of A-62176. AG and TC represent the purine- and pyrimidine-specific chemical cleavage reactions. Lanes 2−5 contain 1, 2, 4, and 8 μM A-62176, respectively, with 10 ng of DNA and 2 mM $MgCl_2$. Brackets A−D correspond to regions of diminished cleavage with DNase I, whereas bracket E shows initially enhanced cleavage. (Right) Densitometric scans of lanes 1−4 of the left panel. The DNA sequence of the lower strand of oligomer 1 is shown in lane 1, and DNase I inhibition (A−D) and enhancement (E) zones are shown in lane 2.

As anticipated, for ethidium bromide and A-85226 in the presence of Mg^{2+}, the DNA contour length ratio increases with increasing ratio of ligand to DNA but reaches a plateau value when saturation binding is attained. For ethidium bromide, the saturation point is at a ratio of 0.45 drug molecules per DNA base pair, while for A-85226, saturation binding occurs at a ratio of 0.80 drug molecules per DNA base pair. The contour length ratio of DNA reaches a plateau value of 1.09 at a drug:DNA base pair ratio of 0.45 for a classical intercalator like ethidium bromide. Significantly, a similar value is obtained for A-85226 in the presence of Mg^{2+} (25 mM) at the same drug:DNA ratio (point at which the lines cross in Figure 8). In the absence of Mg^{2+}, addition of A-85226 to calf thymus DNA initially causes a decrease in contour length, and this is followed by a slow increase in contour length as more drug is added.

The viscometric results provide excellent evidence that the quinobenzoxazine−Mg^{2+} complex is an intercalator and that it increases the contour length of DNA in a similar way to ethidium bromide, although the final stoichiometry (drug:DNA base pair) is apparently different. However, in the absence of Mg^{2+}, the contour length of DNA is not affected by addition of drug, indicating that drug binding involves an alternative mechanism, such as minor groove or an external binding mode.

(iii) NMR Experiments. The effects on the low-field ^{1}H-NMR spectra of DNA upon addition of DNA ligands are a diagnostic tool for deducing ligand binding modes. For intercalators, upfield shifts of imino protons are often observed, which are accompanied by some broadening of the resonance envelopes. In contrast, downfield shifts of imino resonances are characteristic of groove binders.[28]

Figure 9 (panel A) shows the low-field NMR spectra of a magnesium-containing solution of $[d(G\text{-}C)_5]_2$ as a function of increasing amounts of A-85226. The presence of resonances due to the H-bonded imino protons of the G residues of $[d(G\text{-}C)_5]_2$ in H_2O demonstrates that the oligomers are in the duplex form.[29] As drug is added to a solution of $[d(G\text{-}C)_5]_2$, a new peak appears at 12.62 ppm, and the resonances at 13.00 and 13.15 ppm decrease in intensity (scans a−e). At relatively high drug levels (scan e, ratio of DNA to drug is 1:2), even the originally most downfield resonance signal shifts slightly upfield. These spectral effects are indicative of an intercalative binding mode.

In contrast, a quite different result is obtained for the $[d(A\text{-}T)_5]_2$ titration experiment with A-85226 in the presence of Mg^{2+} (Figure 9, panel B). As A-85226 is

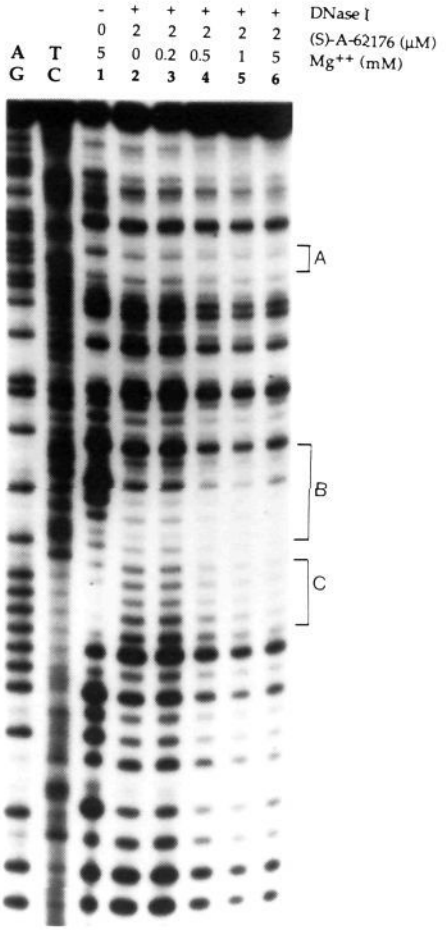

Figure 6. Effect of increasing concentrations of Mg^{2+} on the DNase I footprinting of oligomer 2 (for sequence, see Experimental Section) in the presence of 2 μM A-62176. Lanes 1–6 contain 5, 0, 0.2, 0.5, 1, and 5 mM $MgCl_2$, respectively. Lane 1 contains 7 ng of DNA but without A-62176. Lanes 2–6 contain 7 ng of DNA with 2 μM A-62176 in 20 μL of a solution containing 10 mM Tris-HCl (pH 7.6) and 10 mM NaCl. Brackets A–C correspond to three sites of inhibition of DNase I cleavage (5′-CGA, 5′-TTGCT, and 5′-AAAGC, respectively).

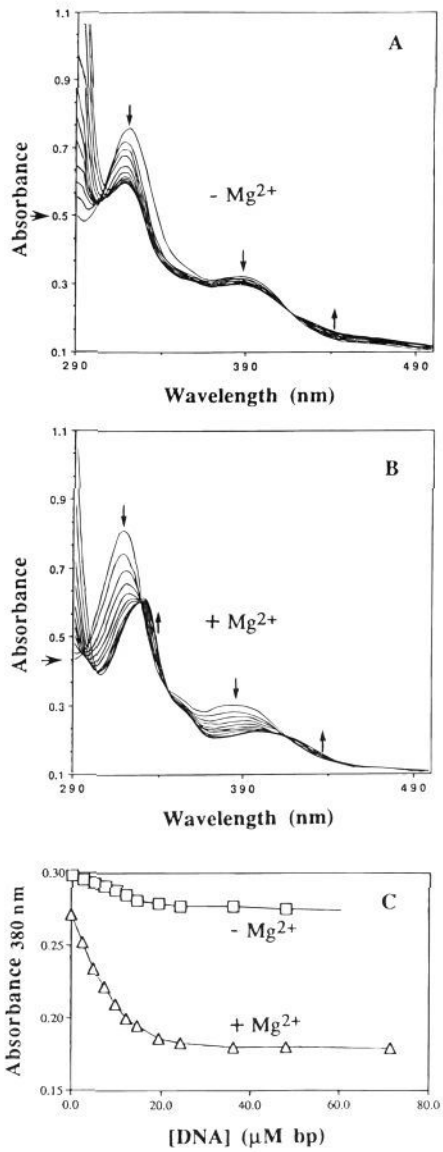

Figure 7. Effect of increasing DNA concentrations on the UV absorption (arbitrary unit) of A-62176 in the absence (panel A) and presence (panel B) of 10 mM Mg^{2+} at room temperature. The absorbance changes at 380 nm as a function of increasing concentrations of DNA in the presence and absence of Mg^{2+} are shown in panel C. The arrows on the *y* axis of panels A and B indicate the spectrum of the drug in the absence of DNA.

added to a magnesium-containing solution of $[d(A\text{-}T)_5]_2$, new resonance signals do not appear. The imino proton signals broaden but shift less than 0.1 ppm (compare scans a and d). By UV spectrophotometry, A-85226 has been shown to bind to $[d(A\text{-}T)_5]_2$ in the presence of magnesium, since the UV spectrum shows a red shift and clear isobestic points during the titration of A-85226 by DNA (data not shown). Therefore, the peak broadening observed in the NMR titration experiment (panel B) suggests that A-85226 binds to the outside of $[d(A\text{-}T)_5]_2$ in a nonspecific manner, possibly by electrostatic interactions with the phosphate backbone.[28,30]

The spectral changes of the ternary $[d(A_4GCT_4)]_2$–Mg^{2+}–A-85226 complexes as a function of increasing drug:DNA ratio are shown in Figure 9 (panel C). Initial additions of drug up to a drug:DNA ratio of 1:1 produce upfield shifts for GC imino proton resonances from 12.8 to 12.5 ppm, while the chemical shifts of the A-tract imino proton resonances remain unchanged (compare scans a and c). When excess drug is added (DNA:drug ratio of 1:2), the A-tract imino proton peaks broaden and move upfield, while the GC imino proton resonances shift further upfield to 12.4 ppm (scan d). This result clearly shows that the quinobenzoxazines preferentially intercalate in the GC region. However, once intercalation of GC base pairs occurs, further drug intercalation in the A-tract region follows.

Mg^{2+} Bridges the Quinobenzoxazine Molecule to the Phosphate Backbone of DNA. Palumbo and coworkers[5,18] have suggested that the quinolone antibiotics may interact with the phosphate of single-stranded DNA via a bridging Mg^{2+} ion. To explore whether the quinobenzoxazine antineoplastics are bridged via an Mg^{2+} ion to the DNA phosphate backbone, the ^{31}P-NMR spectral changes of $[d(G\text{-}C)_5]_2$ in the presence of A-85226 and Mg^{2+} were studied.

Figure 10 shows the ^{31}P-NMR spectra of $[d(G\text{-}C)_5]_2$ in the presence and absence of A-85226 in NMR buffer (10 mM NaH_2PO_4 and 100 mM NaCl) containing 100 mM $MgCl_2$. A single resonance signal at −0.88 ppm for all the phosphate groups is observed for $[d(G\text{-}C)_5]_2$

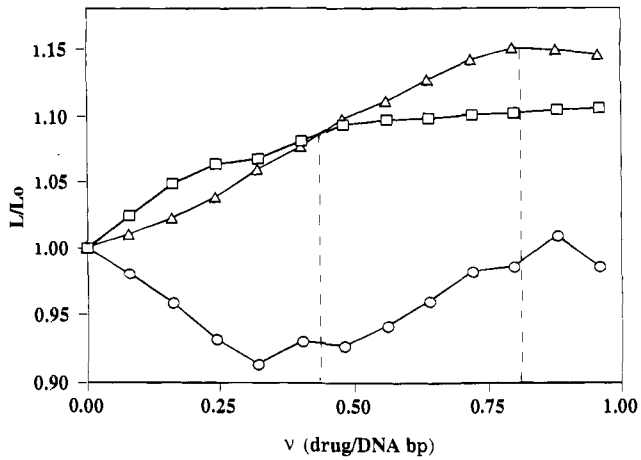

Figure 8. Viscometric titration of sonicated calf thymus DNA with ethidium bromide and A-85226 in the presence and absence of Mg^{2+} (25 mM) at 22 °C in 0.01 M Tris buffer. The ratio of the contour length of DNA, L/L_0, is plotted as a function of moles of drug added per mole of DNA base pairs, ν. The vertical dotted lines show the intercepts on the x axis where the ethidium bromide and A-85226 (Mg^{2+}) plots intersect. (−△−) = A-85226 + Mg^{2+}; (−○−) = A-85226; and (−□−) = ethidium bromide.

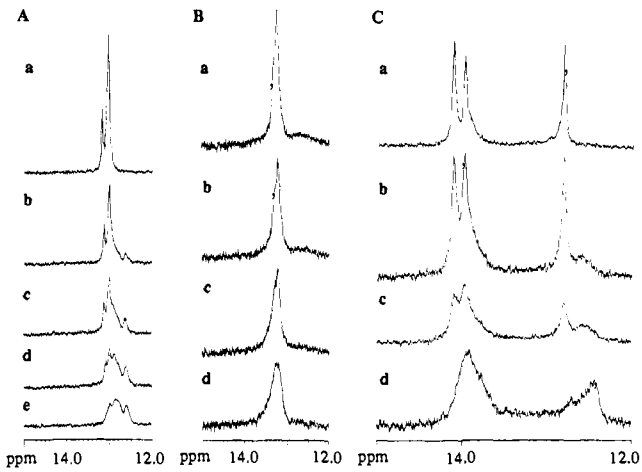

Figure 9. Low-field ^{1}H-NMR spectra showing the effect of addition of A-85226 on the imino proton signals of three synthetic DNA oligomers. The DNA concentration is 1 mM in 10 mM NaH_2PO_4, 100 mM NaCl, 100 mM $MgCl_2$ in 9:1 H_2O:D_2O. (A) $[d(G\text{-}C)_5]_2$:A-86226 ratios of (a) 1:0, (b) 1:0.5, (c) 1:1, (d) 1:1.5, and (e) 1:2 are shown. (B) $[d(A\text{-}T)_5]_2$:A-86226 ratios of (a) 1:0, (b) 1:0.5, (c) 1:1, and (d) 1:2 are shown. (C) $[d(A_4GCT_4)]_2$:A-86226 ratios of (a) 1:0, (b) 1:0.5, (c) 1:1, and (d) 1:2 are shown.

(Figure 10A). However, upon addition of A-85226 to the $[d(G\text{-}C)_5]_2$ solution, two new resonance signals in the downfield region between −0.72 and −0.10 ppm appear (Figure 10C). For comparison, the intercalator ethidium bromide was also used in this study. Upon addition of ethidium bromide to the $[d(G\text{-}C)_5]_2$ oligomer, just one new resonance signal at −0.68 ppm is observed, presumably due to conformational changes on the DNA phosphate backbone induced by intercalation of ethidium bromide into DNA (Figure 10B). This appearance of a new signal slightly downfield from the DNA backbone ^{31}P resonance has been observed in previous studies of DNA−intercalator complexes[31-33] and reflects the local distortion of the backbone that occurs due to formation of the intercalating complex. Significantly, for both ethidium bromide and A-85226, distinct signals

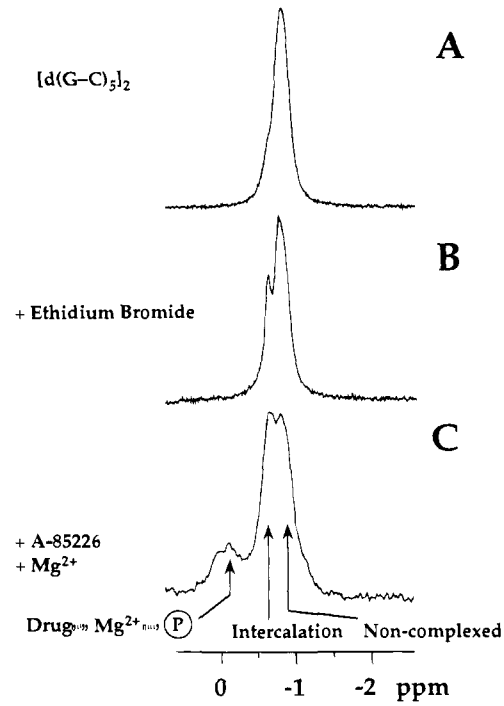

Figure 10. ^{31}P-NMR spectra of $[d(G\text{-}C)_5]_2$ (A) and $[d(G\text{-}C)_5]_2$ in the presence of ethidium bromide (B) and A-85226 (C). For B and C, the mole ratios of oligomer to drug were 1:2. The oligomer (drug) complexes were dissolved in NMR buffer (10 mM NaH_2PO_4 and 100 mM NaCl) and 100 mM $MgCl_2$ at 27 °C in 100% D_2O.

are seen for both unperturbed and unwound phosphate backbone ^{31}P resonances, indicating that the exchange between intercalated and free DNA sites is slow on the ^{31}P-NMR time scale for these ligands. Since in the present study the quinobenzoxazine−Mg^{2+} complexes have been confirmed as intercalators, the new downfield signal at −0.72 ppm in Figure 10B can be attributed to intercalation. However, the additional ^{31}P-NMR resonance signal at −0.10 ppm, which is unique to the A-85226−Mg^{2+}−$[d(G\text{-}C)_5]_2$ complex, cannot be explained by either purely intercalation or groove binding. The resonance signal at −0.10 ppm must be due to a different effect and is consistent with a distortion of the deoxyribose phosphate backbone due to formation of an A-62176−Mg^{2+}−(oxygen)phosphate coordination complex.

A-62176 Has GC Base Pair Preference at Substitution Levels of Drug and Interacts in a Cooperative Manner with DNA. The previously described DNase I footprinting experiments (Figures 5 and 6) and the ^{1}H-NMR results (Figure 9) demonstrate the GC base pair binding preference of the quinobenzoxazines. In order to quantify this preference, association constants for binding of A-62176 to various DNA oligomers were measured spectrophotometrically. The Scatchard plots for A-62176 bound to poly[d(G-C)$_2$] and poly[d(A-T)$_2$] in the presence of 10 mM $MgCl_2$ are shown in Figure 11. The solid lines drawn through the data represent the best fit using the Scatchard equation.[34] Under identical conditions, A-62176 binds more strongly to poly[d(G-C)$_2$] than it does to poly[d(A-T)$_2$], and the association constants for the drug binding to poly[d(G-C)$_2$] and poly[d(A-T)$_2$] are 6.1×10^5 and 3.8×10^5 M^{-1}, respectively. These results confirm that the A-62176−Mg^{2+} complex binds preferentially to GC-rich regions in double-

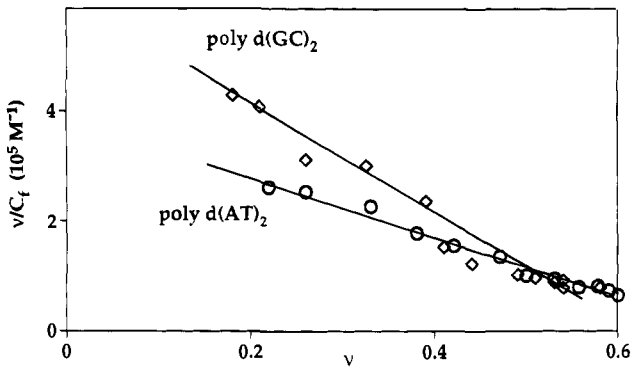

Figure 11. Scatchard plot of A-62176 binding to poly[d(G-C)$_2$] (–□–) and poly[d(A-T)$_2$] (–○–) in the presence of $MgCl_2$ (10 mM).

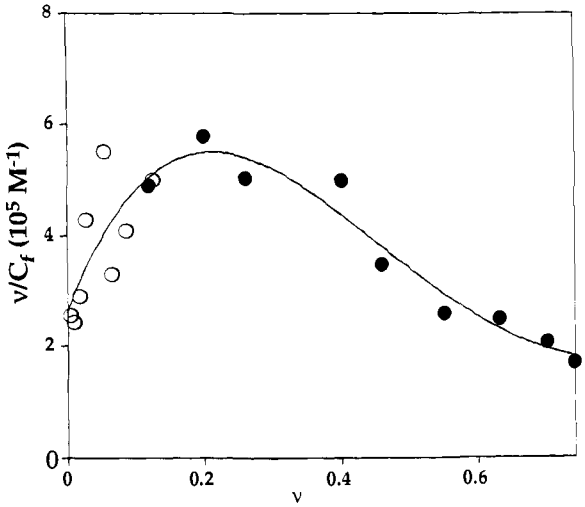

Figure 12. Scatchard plot of combined data from equilibrium dialysis fluorescence emission at 500 nm (open circles) and spectrophotometric titration absorption at 380 nm (closed circles) for A-62176 binding to calf thymus DNA.

stranded DNA, as would be expected for a typical intercalator.

As shown in Figure 11, spectrophotometric titration failed to produce data for $\nu < 0.2$. In this low-binding region, addition of more DNA causes only very small changes in absorbance (Figure 7) and therefore is not suitable for calculating the bound and free drug concentrations. Equilibrium dialysis can overcome this problem by separating the free drug and the drug–DNA complex into two compartments. Free drug concentration can be measured by the intrinsic fluorescence of the drug. However, at high-binding ratios ($\nu > 0.3$), free drug becomes more concentrated, and the prolonged time periods needed for reaching equilibrium cause the drug to precipitate. Therefore, the two methods were combined to obtain a complete Scatchard plot.

A Scatchard plot obtained by combining data from both sources for A-62176 binding to calf thymus DNA generates a smooth isotherm with a maximum near $\nu = 0.2$ (Figure 12). Fitting the combined data to the McGhee and von Hippel model[35] gives an association constant (k) of $3.5 \pm 0.4 \times 10^5\ M^{-1}$ with a cooperativity parameter (w) of 3.2 ± 0.6 and a binding site size (n) of 1.27 ± 0.06. A value for w of >1 is associated with positive cooperativity, and the binding site size fits well with the viscometry measurements (see Figure 8). Not unexpectedly, there was also a systematic deviation of data from the best fit. In the model proposed (see later) for the quinobenzoxazine–Mg^{2+}–DNA complex involving multiple interactions between drug molecules in different environments, it is not surprising that the model does not adequately describe the experimental system. Therefore, the McGhee and von Hippel model is only used to *qualitatively* show the positive cooperativity effect. This result confirms our expectations from the DNase I footprinting experiments (see Figure 5) that binding of a first drug molecule creates better binding sites for other drug molecules.

4. Norfloxacin Enhances the DNase I Footprint Generated by A-62176 in the Presence of Mg^{2+} and Produces a Greater DNA Lengthening Effect with A-62176 as Determined by Viscometry. Since both Norfloxacin and the quinobenzoxazine antitumor agents require Mg^{2+} for interaction with DNA, but only the quinobenzoxazines can form a stable intercalation complex with duplex DNA, the possibility of a cooperative binding to DNA by the two compounds was evaluated. The DNase I footprinting patterns of A-62176 alone (lanes 2–5), Norfloxacin alone (lane 7), and the two combined drugs (lanes 8–11) are shown in Figure 13, top. As anticipated, Norfloxacin alone is invisible to DNase I footprinting (compares lanes 6 and 7), while increasing concentrations of A-62176 initially inhibit DNase I cleavage of GC-rich regions with associated unwinding and enhanced cleavage of the AT-rich regions (lanes 2–4). These AT regions are themselves inhibited from DNase I cleavage at the highest drug concentration (lane 5). The effect of a constant amount of Norfloxacin (15 μM) on the DNase I footprinting pattern of A-62176 is shown in lanes 8–11. While this concentration of Norfloxacin alone does not inhibit the DNase I cleavage pattern, in combination with A-62176 there is enhancement of the footprinting strength of the quinobenzoxazine antineoplastic agent A-62176. This is most clearly shown by comparing the densitometric scans of lanes 4 and 10 (scans A and C in Figure 13, bottom) with those of lanes 5 and 11 (scans B and D in the bottom panel), respectively. Addition of 15 μM Norfloxacin to 2 μM A-62176 (lane 10 in the top panel and scan C in the bottom panel) results in a DNase I footprinting pattern that is almost equivalent to that obtained with 4 μM A-62176 (lane 5 in the top panel and scan B in the bottom panel). The results of these experiments suggest that, although less potent than A-62176, Norfloxacin can interact cooperatively with A-62176.

If Norfloxacin and A-62176 can cooperatively interact with DNA in the presence of Mg^{2+}, as suggested by the DNase I footprinting experiments, then together they should have an additive effect on lengthening of the DNA helix. To test this postulate, viscometric titration profiles of the contour length ratio of DNA (L/L_0) against moles of drug adduct per mole of DNA base pair were carried out for A-85226 alone, Norfloxacin alone, and a 1:1 mixture of both in the presence of Mg^{2+}. The results shown in Figure 14 demonstrate that while Norfloxacin alone shows no lengthening effect on DNA the 1:1 mixture of Norfloxacin and A-85226 shows an additive lengthening effect that parallels the effect of pure A-85226 at twice the concentration of quinobenzoxzine present in the 1:1 Norfloxacin:A-85226 mixture. Interestingly, the 1:1 mixture of Norfloxacin and A-85226

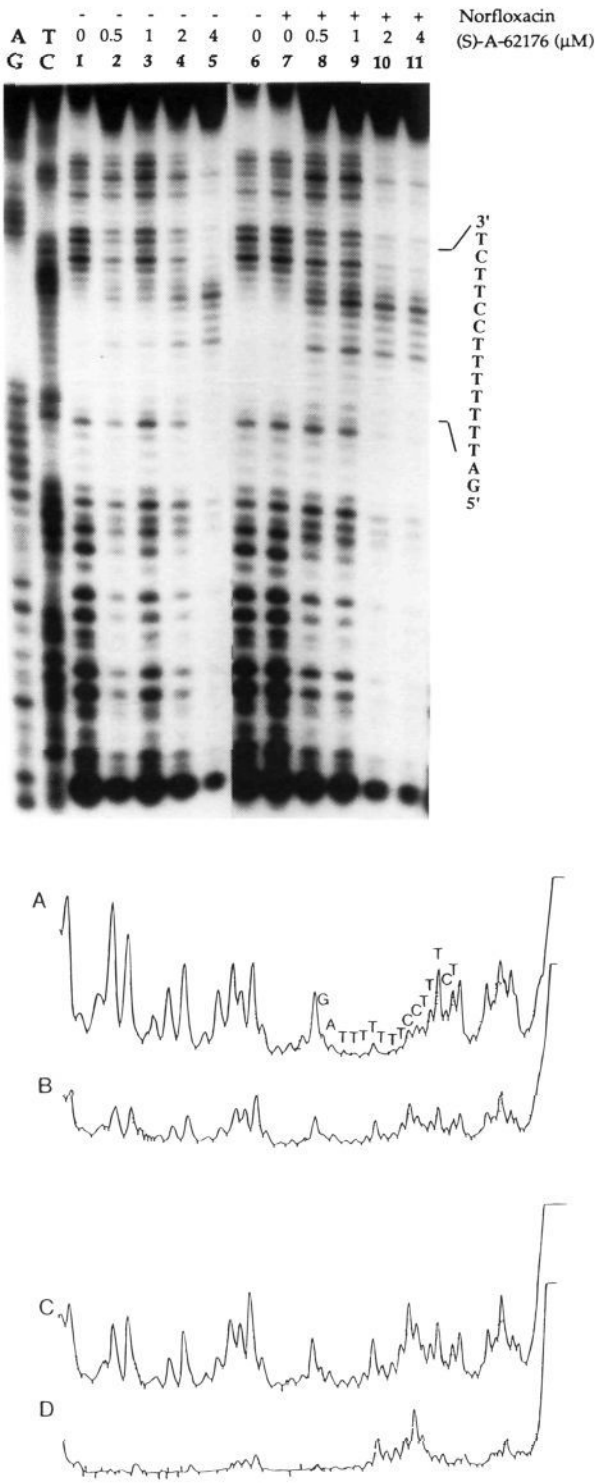

Figure 13. (Top) Effect of Norfloxacin on the DNase I footprinting of A-62176 with oligomer 1 (for sequence, see Experimental Section). Lanes 1–5 contain 0, 0.5, 1, 2, and 4 μM A-62176, respectively, with 20 ng of DNA in 20 μL of solution containing 10 mM Tris-HCl (pH 7.6), 2 mM $MgCl_2$, and 10 mM NaCl. For lanes 7–11, 15 μM Norfloxacin was preincubated with 0, 0.5, 1, 2, and 4 μM A-62176, respectively, in the same buffer solution for 10 min, and 20 ng of DNA (oligomer 1) was then added to the reaction mixtures. Lane 6 is identical with lane 1. AG and TC represent the purine- and pyrimidine-specific chemical cleavage reactions. The sequence of the DNase-enhanced region is shown to the right. (*Bottom*) Densitometric scans of lanes 3, 4, 9, and 10 of the top panel are shown in panels A–D, respectively.

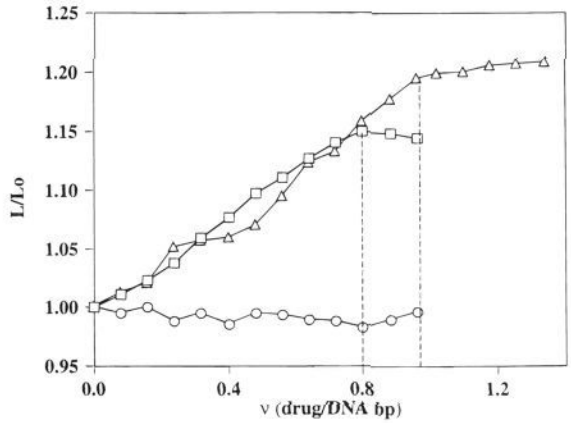

Figure 14. Viscometric titration of sonicated calf thymus DNA with A-85226, Norfloxacin, and a 1:1 mixture of A-85226 and Norfloxacin in the presence of Mg^{2+} (25 mM) at 22 °C in 0.01 M Tris buffer. The ratio of the contour length of DNA, L/L_0, is plotted as a function of moles of drug added per moles of DNA base pairs, ν. The vertical dotted lines show the intercepts (0.80 and 0.96) on the x axis for where saturation binding of A-85226 (Mg^{2+}) and A-85226 and Norfloxacin is attained, respectively. (−△−) = A-85226 + Norfloxacin (1:1); (−□−) = A-85226; and (−○−) = Norfloxacin.

produces an even greater lengthening effect than A-85226 alone (i.e., a final drug to DNA ratio (ν) of almost 1 vs 0.8 for A-85226 alone). This result, when taken in conjunction with the DNase I footprinting experiment (Figure 13), demonstrates that Norfloxacin and the quinobenzoxazines bind to DNA in a cooperative manner.[36]

5. The Intercalative Binding Drugs Ethidium Bromide and Echinomycin Cannot Substitute for A-62176 in the Cooperative Interaction of Norfloxacin with DNA in the Presence of Mg^{2+}. Based upon the data described above, two alternative models for the A-62176–Norfloxacin complex with DNA in the presence of Mg^{2+} ions can be proposed. In the first model, A-62176 and Norfloxacin play *similar structural* roles in the interaction with DNA. However, the ability of Norfloxacin to interact with DNA is dependent upon initial intercalative binding by A-62176, which results in local unwinding of DNA, thereby providing a destabilized adjacent site for stable intercalative binding by Norfloxacin. In the second case, A-62176 and Norfloxacin play *dissimilar structural* roles in the interaction with DNA. In this case, A-62176 is uniquely responsible for the intercalative role and Norfloxacin plays a nonintercalative role in the complex but is still structurally dependent upon A-62176 and Mg^{2+} for interaction with DNA. *The two models can be differentiated by testing* the general role of intercalation in creating binding sites on DNA for Norfloxacin. If the sole purpose of A-62176 is to provide destabilized intercalation sites for Norfloxacin through intercalation, then structurally unrelated intercalating agents such as ethidium bromide or echinomycin should be able to substitute for A-62176. Conversely, if Norfloxacin does not itself intercalate but rather interacts with DNA in a manner that is dependent upon both Mg^{2+} and A-62176, then simple intercalation per se will be insufficient to provide a cooperative interaction with Norfloxacin. Parallel experiments to those described before (using DNase I footprinting and viscometry) but using echinomycin and ethidium bromide, respectively, in place of A-62176 were carred out

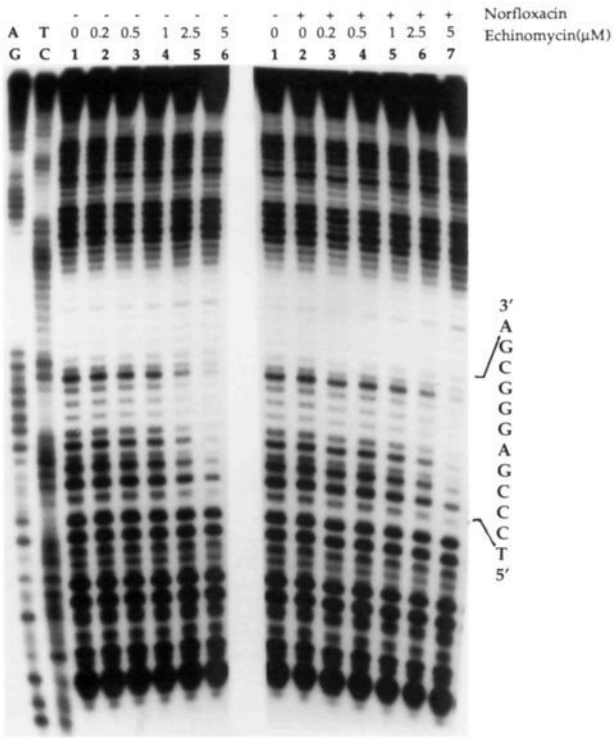

Figure 15. Effect of Norfloxacin on the DNase I footprinting pattern of echinomycin. Lanes 1−6 and 2−7 in the left and right panels, respectively, are the same incremental increasing concentrations of echinomycin, and in the right panel only, lanes 2−7 contain Norfloxacin (15 μM). AG and TC represent the purine- and pyrimidine-specific chemical cleavage reactions. The sequence to the right of lane 7 corresponds to the echinomycin DNase I footprint.

with Norfloxacin. The results of the DNase I footprinting experiments (see Figure 15) show that echinomycin is unable to provide an additive effect on inhibition of DNase I footprinting, despite the documented ability of similar bis-intercalators[37] to produce local unwinding of DNA (compare lanes 1−6 in the left panel with lanes 3−7 in the right panel in Figure 15, which have the same concentrations of echinomycin but in the presence or absence of Norfloxacin). The viscometry experiments also show that Norfloxacin was unable to provide an additive lengthening effect on DNA in the presence of ethidium bromide (data not shown). Therefore, both sets of results show that mere intercalative binding by echinomycin and ethidium bromide, and thus local unwinding of DNA, is insufficient to provide a local DNA environment suitable for cooperative interactions with Norfloxacin. This argues strongly against the first model, in which Norfloxacin and the intercalators would play interchangeable roles. Rather, this data is consistent with a second model, in which A-62176 exclusively provides the intercalative binding moiety and also plays an additional structural role in interacting with Mg^{2+} and Norfloxacin. In a subsequent experiment, in which the descarboxyl A-62176 was used in conjunction with Norfloxacin, no cooperative effect was observed, even though the descarboxyl compound is able to weakly intercalate with DNA (data not shown). This provides additional evidence for the importance of the β-keto acid in providing stabilization of the drug:Mg^{2+} complex in the cooperative intercalation with Norfloxacin.

Discussion

The quinobenzoxazine antineoplastic agents bear strong structural similarities to the quinolone antibiotics typified by Norfloxacin (see Figure 1). Indeed, the design of these compounds was inspired by the structure of Norfloxacin-type compounds that are clinically useful antibacterial compounds. Surprisingly, while the quinobenzoxazine compounds lacked significant antibacterial activity, they did have antineoplastic activity that was dependent upon the presence of divalent cations, such as Mg^{2+} and Mn^{2+}.[2] This latter observation was significant because although the biological activities were different, both the quinobenzoxazines (data shown here) and the quinolones[18] exhibit a requirement for Mg^{2+}. The subsequent observation reported here that, while the quinolones do not appear to form stable complexes with duplex DNA, the quinobenzoxazines were able to do so in the presence of Mg^{2+} suggested that stable complexation with *duplex* DNA might be the basis for departure from antibacterial to antineoplastic activity. These preliminary observations inspire two related questions: (1) what is the structure of the quinobenzoxazine−Mg^{2+} complex with duplex DNA that is presumably responsible for the catalytic inhibition of topoisomerase II activity and antineoplastic activity and (2) what is the structural relationship between the ternary quinobenzoxazine−Mg^{2+}−DNA complex and the quaternary quinolone−Mg^{2+}−DNA−gyrase complex? The results reported here, together with the recently proposed Palumbo model for the quinolone−Mg^{2+}−phosphate chelation complex,[5] provide the basis for a revised model for the quinolone−Mg^{2+}−DNA−gyrase complex and important insights into the design of new quinolone antibacterial agents, as well as a proposed structure for the quinobenzoxazine−Mg^{2+}−DNA complex.

Determination of the Structure of the Quinobenzoxazine−Mg^{2+}/Mn^{2+} Complex. The well-established ability of the antibacterial quinolones to bind to di- and trivalent metal ions has led us to investigate the ability of the related quinobenzoxazines to bind manganese and magnesium ions. The formation and structure of the quinobenzoxazine−metal ion complexes were characterized by FT-IR and agarose gel electrophoresis experiments. The FT-IR results clearly implicate the 5-carboxylate moiety of the quinobenzoxazines in magnesium complexation, although definitive proof is still lacking. Although we have no unequivocal evidence for the role of the 4-keto group in complexation, we favor a model in which the 4-keto group of the quinobenzoxazines participates, in combination with the 5-carboxylate group, in chelation of the divalent metal ion. This model is consistent with the invariant nature of the 4-keto group in the closely related antibacterial quinolones. Mendoza-Diaz and co-workers[38] have shown by X-ray crystallography that the 4-keto group of nalidixic acid is involved in the complexation of this quinolone with Cu^{2+}-phenanthroline.[39] We note that there are other, unassigned bands unique to the IR spectrum of the quinobenzoxazine−Mg^{2+} complex (~1000 cm^{-1}, Figure 3, upper spectrum) that may indicate that additional functional groups of the drug are involved in complexation with magnesium. Potential sites for complexation include the amino substituent of the C-1 pyrrolidine moiety.

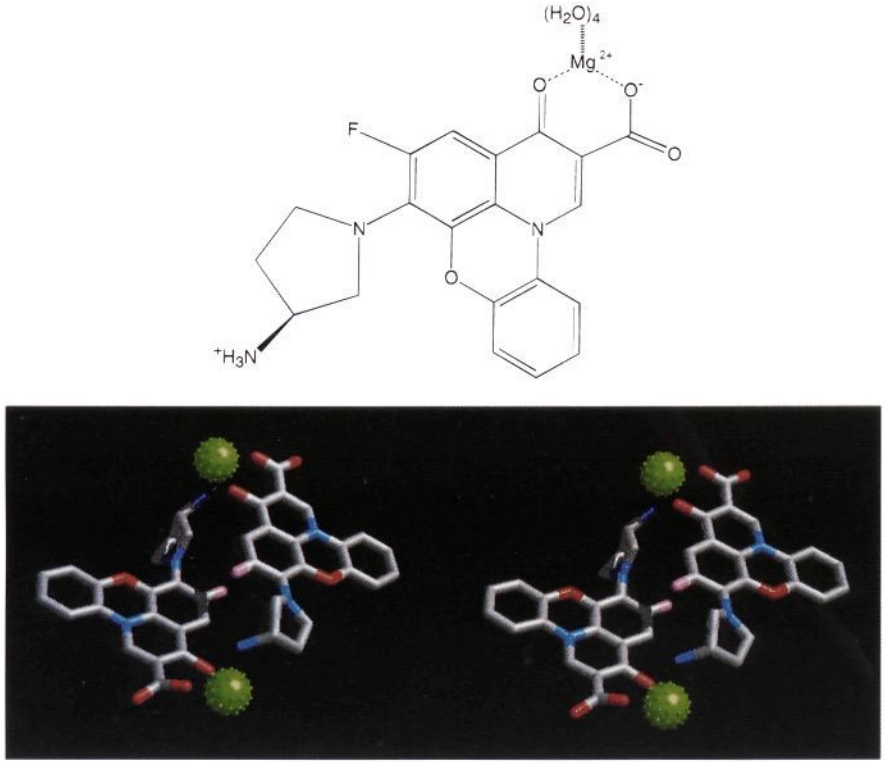

Figure 16. Proposed structures of the 1:1 (top) and 2:2 (bottom) A-62176:Mg^{2+} complexes. In the 2:2 complex, stereodiagrams of the head-to-tail complexes are shown.

Both the quinobenzoxazine–Mn^{2+} and quinobenzoxazine–Mg^{2+} complexes migrate during gel electrophoresis (Figure 2). The Mg^{2+} and Mn^{2+} ions have similar ionic radii (0.065 and 0.080 nm, respectively)[40] and, excluding redox reactions, are chemically similar. Evidence from FT-IR with supportive data from ^{1}H- and ^{13}C-NMR spectra (unpublished results) suggests that both metal ions bind to the ketonic carbonyl and carboxyl moieties of the quinobenzoxazine compounds, as shown in Figure 16. We therefore have used the *more tightly binding manganese ion in a Job titration* to determine the stoichiometry of the quinobenzoxazine–metal complex. The Job titration confirms that the quinobenzoxazine–Mn^{2+} complex forms in an equimolar ratio, e.g., 1:1, 2:2, etc. By extension, the quinobenzoxazine–Mg^{2+} complex also forms a similar positively charged complex.

The combined results of the gel electrophoresis, FT-IR, and Job titration experiments suggest that a quinobenzoxazine–Mg^{2+} complex forms in equimolar proportions between the drug and divalent cation. The simplest complexation would involve a 1:1 ratio of drug to Mg^{2+} (Figure 16, top), but for reasons discussed later, we favor the alternative 2:2 complex of drug to Mg^{2+}, in which two drug molecules form a head-to-tail complexation with two Mg^{2+} ions. In such a 2:2 quinobenzoxazine–Mg^{2+} complex, each drug molecule could participate in Mg^{2+} complexation, with the β-keto acid and the amino group of two different drug molecules serving as ligands for each of the two magnesium ions (see Figure 16, bottom). Such a 2:2 complex has previously been proposed, on the basis of spectrofluorimetric studies, for the interaction between the antibacterial fluoroquinolones and magnesium ions.[41]

Magnesium Ions Play an Important Role in the Interaction of the Quinobenzoxazines with DNA. To investigate the role of Mg^{2+} in the interaction of the quinobenzoxazines with DNA, we employed UV–vis spectroscopy to study the interaction of quinobenzoxazines with calf thymus DNA in the presence and absence of magnesium. In the absence of magnesium, the quinobenzoxazines appear to interact with DNA in a relatively weak, nonselective fashion. There are modest changes in the UV region of the absorption spectrum of A-62176 with added DNA in the absence of magnesium, but the lack of a clear isobestic point indicates a multitude of binding modes. In contrast, in the presence of magnesium, a number of marked changes occur in the absorption spectra of A-62176 upon addition of DNA. There are bathochromic shifts in both the UV and visible regions of the spectrum of the drug and clear isobestic points (compare panels A and B in Figure 7). Upon the basis of these observations, the quinobenzoxazines appear to interact with DNA in quite different ways in the presence and absence of Mg^{2+} ions. A topoisomerase relaxation assay, viscometric titrations, and NMR evidence clearly indicate that the magnesium-dependent DNA binding of the quinobenzoxazines involves intercalation; we assume that the magnesium-independent binding involves interaction with the grooves or exterior of the DNA double helix. The association constant of A-62176 binding to poly[d(G-C)$_2$] in the presence of 10 mM Mg^{2+} was determined to be 6.1×10^5 M^{-1}. This magnesium-dependent interaction of quinobenzoxazines with linear double-stranded DNA is to be contrasted to the antibacterial quinolones, which only bind to supercoiled circular DNA, not linear double-stranded DNA, in the presence of magnesium. Furthermore, the association constant for the magnesium-

dependent binding of A-62176 to calf thymus DNA that we report is an order of magnitude higher than the association constant previously reported for Norfloxacin binding to supercoiled DNA in the presence of magnesium (4.2×10^4 M^{-1}).[18]

Determination of the Structure of the Quinobenzoxazine–Mg^{2+} Complex with DNA. Spectroscopic (UV, CD, NMR) and other experimental methods (viscometry, gel electrophoresis) were used to explore the nature of the ternary complex between the quinobenzoxazines, Mg^{2+}, and DNA. The results of these studies provide insights into the sequence specificity of the drug–DNA binding reactions and a detailed characterization of the quinobenzoxazine–Mg^{2+}–DNA complex, ligand-induced conformational transitions in DNA, the stoichiometry of the drug–Mg^{2+}–DNA complex, and cooperativity in drug binding.

Previous studies have shown that when the concentration of Mg^{2+} in the solution is greater than 0.7 M, or the concentration of Na^+ is greater than 2 M, the conformation of DNA is changed from B- to Z-form.[42] Thus, reaction conditions throughout this study are carefully selected in order to avoid conformational changes in DNA induced by high salt concentration. The CD spectral changes (unpublished results) observed upon addition of the quinobenzoxazines to poly[d(G-C)$_2$] confirm the importance of Mg^{2+} in facilitating the interaction of A-85226 with DNA and also show that the DNA remains in B-form DNA throughout the titration process in both the presence and absence of 10 mM $MgCl_2$.

There is clear evidence that in the presence of magnesium the quinobenzoxazines intercalate into double-stranded DNA: quinobenzoxazine binding is accompanied by unwinding of closed circular DNA, as determined in the topoisomerase assay, by lengthening and stiffening of linear double-stranded DNA, as determined by viscometric studies, and by downfield shifts of the phosphorus signals and upfield shift of the imino proton signals in the NMR. Additional information concerning the nature of the intercalation complex formed between quinobenzoxazine, Mg^{2+}, and DNA was also obtained from these studies.

In contrast to the quinolone gyrase inhibitors, the quinobenzoxazines form a stable complex with duplex DNA. Therefore, we were able to probe directly the interaction of the quinobenzoxazines with DNA, using ^{31}P-NMR to address the possibility of a drug–phosphate bridging role for Mg^{2+}. The results show that at subsaturating levels of drug three ^{31}P-NMR signals are present. The most upfield (−0.88 ppm in Figure 10C) is assigned to those phosphates in the backbone at which drug modification has not occurred. The downfield chemical shift of the middle ^{31}P-NMR signal (−0.72 ppm) is typical for phosphates at which intercalation has occurred. The remaining most downfield ^{31}P-NMR signal (−0.10 ppm) is unique to the intercalating quinobenzoxazines, which require Mg^{2+} for their binding to DNA. We propose that this downfield-shifted signal is due to the Mg^{2+}-chelated phosphate in which the chelation produces an additional distortive effect on the deoxyribose phosphate backbone.

Several lines of evidence point toward a GC preference for the initial intercalative binding complex of the quinobenzoxazine–Mg^{2+} complex. First, the Scatchard plots show that the association constants for drug binding to poly[d(G-C)$_2$] and poly[d(A-T)$_2$] are 6.1×10^5 and 3.8×10^5 M^{-1}, respectively. The initial DNase I footprints of A-62176 reveal a clear GC preference. Proton NMR studies of the magnesium-dependent interaction of the quinobenzoxazines with various double-stranded DNA oligomers have proved to be especially insightful. The interaction of A-85226 with [d(G-C)$_5$]$_2$ clearly demonstrates intercalation, as evidenced by upfield shifts in the imino proton signals. In contrast, with [d(A-T)$_5$]$_2$, there is no indication of intercalation under similar conditions. Remarkably, with the oligomer [d(A$_4$GCT$_4$)]$_2$, initial intercalation at the GC step is followed by intercalation at the AT base pairs. Thus, while isolated AT base pairs cannot serve as intercalation sites for A-85226, AT base pairs flanking a favored CG site can serve as intercalation sites, clearly demonstrating the cooperativity in the DNA binding by quinobenzoxazines. A parallel result is evident in the DNase I footprinting experiments, where the initial footprint occurs at GC-rich regions, and only after drug binding has occurred at these regions does the adjacent A-tract become receptive to drug binding (Figure 5). We note that there is additional information in the DNase I footprinting experiments that indicates some distortion of A-tract regions flanked by quinobenzoxazine-intercalated GC-rich regions (regions B and E in Figure 5). As expected, the GC-rich regions are cleaved more readily by the DNase I than the A-tract, where little cleavage occurs. However, once intercalation by the quinobenzoxazine has occurred in the GC-rich region, the A-tract becomes susceptible to DNase I cleavage, presumably as a consequence of local unwinding due to intercalation at the adjacent site. Only then, at higher drug concentrations, does this region of drug-induced DNase I cleavage become receptive to intercalation by A-62176. A parallel sequence of events presumably results in the consecutive GC and then AT imino upfield ^{1}H-NMR shifts in the [d(A$_4$GCT$_4$)]$_2$ duplex during titration with A-62176.

A Scatchard plot (Figure 12) shows that A-62176 binds to DNA with a positive cooperativity. The positive binding cooperativity reveals that intercalation of the first drug creates other intercalative sites. The cooperativity can come from two sources: (1) as already mentioned, intercalation in the GC region by A-62176 locally unwinds the adjacent DNA double helix, and this may create better intercalation sites, even within A-tracts, and (2) the aromatic stacking of the externally bounded drug molecule with other drug molecule(s) may initiate and stabilize the intercalation at adjacent sites (see later).

The viscometric titrations demonstrate that the maximal increase in viscosity corresponds to a drug–DNA base pair ratio of ~1:1. This surprising result requires that, at saturation, every base pair step be occupied by an intercalated quinobenzoxazine molecule—in violation of the well-established neighbor exclusion rule.[43] However, if the quinobenzoxazines exist, in the presence of magnesium, as a 2:2 drug–Mg^{2+} complex, and further, if in such a 2:2 complex, only *one* of the two drug chromophores serves as an intercalator, then there is no violation of the neighbor exclusion rule: at saturation only *one* 2:2 quinobenzoxazine–Mg^{2+} dimer is intercalated between *two* base pairs. Minor or major groove

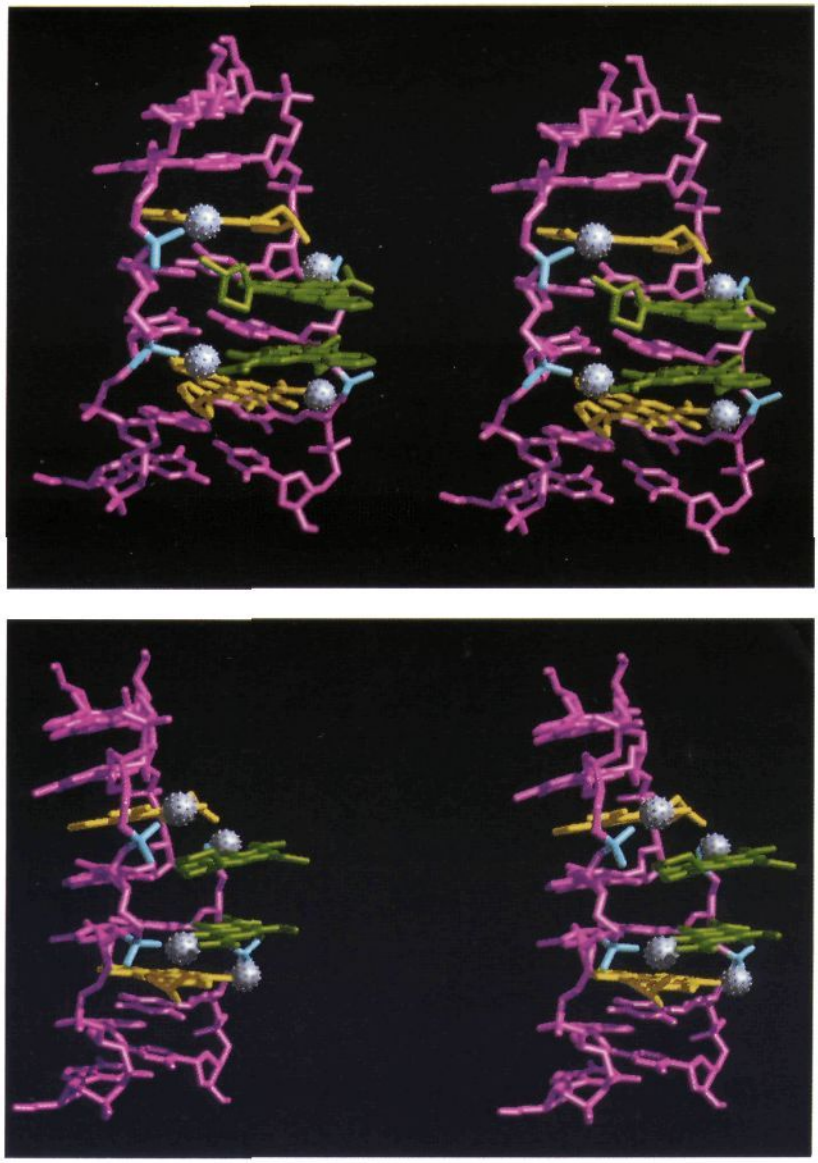

Figure 17. Molecular models of the 4:4 quinobenzoxazine:Mg^{2+} (top) and the 2 + 2:4 mixed quinobenzoxazine/quinolone$-Mg^{2+}-$DNA complexes (bottom). Mg^{2+} ion coordinates with the carbonyl and carboxyl oxygens of the A-62176 molecule and one oxygen on the DNA phosphate backbone, as well as two water molecules. The distances between the Mg^{2+} ion and these coordinated ligands are ~1.72−1.94 Å. The aromatic ring D intercalates between the GC base pairs. In both cases the intercalated A-62176 molecules are shown in yellow, the phosphates involved in the coordination are blue, and the Mg^{2+} ions are gray. The externally bound molecules (A-62176 for the top and Norfloxacin for the bottom) are colored green.

binding can be eliminated for the second drug molecule of the 2:2 complex, since only upfield ^{1}H-NMR shifts of imino protons occur upon formation of the quinobenzoxazine$-Mg^{2+}-$DNA complex. In order to maximize the quinobenzoxazine stacking interactions in the nonintercalated members of the 2:2 complex, two separate 2:2 complexes may arrange themselves so that the externally bound drug molecules are at adjacent positions, but the intercalated moieties are still separated by two base pairs (see Figure 17, top).

Let us examine the data that would support the proposed 2:2 quinobenzoxazine$-Mg^{2+}$ model for the active species involved in intercalation into DNA. Our studies of the A-62176$-Mn^{2+}$ complexation clearly show that a single complex forms with equal molar ratios of metal ion and drug. Previous investigators have proposed a 2:2 drug$-Mg^{2+}$ complex for the closely related antibacterial fluoroquinolones.[41] Thus, our model is consistent with our data on the quinobenzoxazines as well as previously published data on the structurally similar fluoroquinolones. The cooperative nature of the intercalation of quinobenzoxazines can at least be partially attributed to the presence of the "exterior," nonintercalating quinobenzoxazine member of the 2:2 drug$-Mg^{2+}$ complex. The importance of drug−drug interactions in the structure−activity relationship of the antibacterial quinolones has previously been proposed and is supported by a number of X-ray crystal structures of antibacterial quinolones, which show close interactions between neighboring molecules in the crystal lattice.[38] These interactions involve a combination of $\pi-\pi$ stacking and van der Waals contacts between substituents at N-1. We invoke these same interactions, particularly $\pi-\pi$ stacking, to explain how the presence of one intercalated 2:2 complex, with its associated exterior quinobenzoxazine, can facilitate the nearby

intercalation of another 2:2 complex. Drug–drug association between the exterior chromophore of the intercalated 2:2 complex and one of the chromophores of the incoming 2:2 complex will stabilize the intercalation of the incoming 2:2 complex at an intercalation site that might not otherwise be favored. An extension of this rationale dictates that the exterior chromophore of the intercalated 2:2 complex need not be optimized for intercalation but rather must serve only to coordinate the shared magnesium ions in the 2:2 complex and facilitate drug–drug interactions on the exterior of the DNA. We reasoned that the antibacterial quinolones should serve these two functions. Thus, the cooperativity that we observe between the intercalation of the quinobenzoxazines and Norfloxacin is a strong indication that our model is fundamentally correct. Finally, we acknowledge that the principle of self-assembly in designing cytotoxic agents was described some years ago by Rideout.[44] Fortuitously, the self-assembly of the 4:4 drug:Mg^{2+} complex described here on a DNA double helix seems to fulfill the principles proposed in this elegant and clever proposal.

Both the Shen and Palumbo models for the quinolone–DNA interactions have similarities to the 2:1 chromomycin–Mg^{2+} complexes.[45,46] In one case,[14] a self-associated quinolone complex is proposed, and in the other,[5,18] a drug–Mg^{2+} complex is proposed. Conceptually, our thinking about the structure of the quinobenzoxazine–Mg^{2+}–DNA complex was influenced by the existing models for the quinolone–DNA complexes proposed by the Italian group[5] and the U.S. group.[15] Unexpectedly, the cooperative role of A-62176 and Norfloxacin and, conversely, the noncooperative effect of general intercalators such as ethidium bromide were also important observations. Last, the recently reported comparison of the hydroxyl radical footprinting patterns of DNA with the bacterial gyrase, and then after formation of the cleavable complex trapped with a nonhydrolyzable ATP analog or quinolone antibiotic, provided additional crucial insight.[46]

Stereomodels for the proposed 4:4 A-62176–Mg^{2+}–DNA (PO_4) chelation complex are shown in Figure 17, top. This 4:4 complex consists of a pair of 2:2 A-62176–Mg^{2+} dimers. In each 2:2 dimer, the quinobenzoxazine ring D (Figure 1) of one A-62176 molecule is intercalated between the adjacent base pairs and the pyrrolidine ring of this molecule lies in the minor groove, with the amino group coordinating an Mg^{2+} ion that is in proximity to the negatively charged phosphate backbone. Mg^{2+} coordination serves to bridge the amino group of this A-62176 molecule with the carbonyl and carboxyl groups of an adjacent, nonintercalated A-62176 molecule. In a similar way, the carbonyl and carboxyl groups of the intercalated A-62176 molecule coordinate a second Mg^{2+} molecule that is also bound by the amino group of the exterior, nonintercalated A-62176 molecule. Both Mg^{2+} ions of the 2:2 Mg^{2+}:A-62176 complex are also coordinated by the oxygen of the DNA phosphate backbone. The additional coordination sphere about these Mg^{2+} ions is filled with water molecules. Because of steric constraints, it was not possible to form a similar drug–Mg^{2+}–PO_4 complex in the major groove of DNA. Two such 2:2 dimers are then arranged on DNA such that the two externally bound quinobenzoxazines interact through π–π stacking forces and the two intercalated molecules are separated by two base pairs. Stereomodels of an analogous 4:4 mixed A-62176:Norfloxacin dimer Mg^{2+} complex are shown in Figure 17, bottom. In this model, consistent with the results of the cooperativity experiments, the two Norfloxacin molecules are externally bound and the A-62176 molecules are intercalated.

Relationship between the Structure of the 2:2 Quinobenzoxazine–Mg^{2+} Complex with DNA and the Norfloxacin Interaction with the Bacterial Gyrase–DNA Complex. While there are certain similarities between the quinobenzoxazine–DNA and quinolone–gyrase–DNA interactions, there are also critical differences. There is ample evidence that both drugs require Mg^{2+} for their interaction with DNA,[18] and an Mg^{2+} bridged phosphate is implicated. On the other hand, only the quinobenzoxazines are able to form a stable intercalated complex with DNA. Although A-62176 and Norfloxacin are able to form a heterogeneous 2:2 Mg^{2+} complex on DNA (Figure 17, bottom), direct evidence for an intercalative role for Norfloxacin is lacking. The DNA unwinding role of echinomycin at adjacent sites is insufficient to create stable intercalation sites for Norfloxacin, even in the presence of Mg^{2+}. Both the Shen and Palumbo models[5,15] propose that a transient step in the gyrase manipulation of DNA produces a DNA substrate that provides a special niche for the quinolone antibiotics. The two models differ considerably in the precise structure of the substrate binding site and the quinolone complexation species. Upon the basis of the analogies to the 2:2 quinobenzoxazine–Mg^{2+}–DNA complex, we propose a quinolone–Mg^{2+}–phosphate bridge parallel to the Palumbo model[5] but suggest that gyrase-mediated unwinding of *duplex DNA* rather than single-stranded DNA is the more likely target.

Recently, the Maxwell laboratory has determined the hydroxyl radical footprint of DNA in the presence of bacterial gyrase and the quinolones.[47] A comparison of the hydroxyl radical footprinting patterns of DNA with gyrase alone and then after formation of the cleavage complex trapped with a quinolone (CFX) or a nonhydrolyzable ATP analog (ADPNP) shows that the major changes are a shift in the phasing of the cleavage maxima upstream of the cleavage site (i.e., 5′ to the cleavage site on the top strand) and an additional cleavage peak adjacent to the cleavage site (Figure 18). This is common to the footprints found with both the quinolone and nonhydrolyzable ATP analog. We propose that this enhanced cleavage site downstream on both strands is due to transient unwinding of the helix, which is then trapped by intercalation of a Mg^{2+}-stabilized dimer (2:2 model) or pair of dimers (4:4 model) of the quinolones. It is important to recognize that we do not propose the quinolones induce this unwinding but rather that they simply trap the kinetically accessible unwound DNA, since this same enhanced hydroxyl radical cleavage is found in the case of the nonhydrolyzable ATP analog.

Implications for Drug Development. Our model for the structure of the quinobenzoxazine–Mg^{2+}–DNA complex (Figure 17) proposes what is effectively a *heterodimer* of the 2:2 drug–Mg^{2+} complex with respect to the receptor, since while one drug molecule is intercalated the other is externally bound to DNA. In

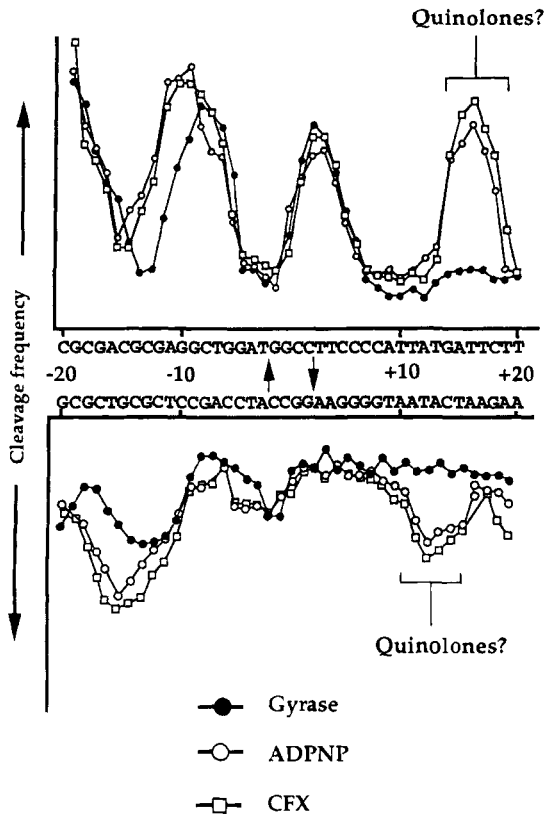

Figure 18. Plots of relative hydroxyl radical cleavage frequency at each nucleotide of duplex DNA in the presence of bacterial gyrase alone (−●−); with ADPNP (5′-adenylyl-β,γ-iminodiphosphate), a nonhydrolyzable ATP analog (−○−); and with CFX (ciprofloxacin), a quinolone antibacterial (−□−) (adapted from Figure 3C in ref 47, with permission). Arrows between the duplex sequences indicate gyrase-induced DNA cleavage sites. The brackets indicate the quinolone antibacterial−Mg^{2+} complex intercalation/external binding site, as proposed by us.

the presumed intracellular target (topoisomerase II for the quinobenzoxazines and bacterial gyrase for the quinolones), this represents *two* distinct targets for the drug molecules. While the intercalated molecule interacts exclusively with DNA, the second externally bound molecule interacts with the protein (topoisomerase II or gyrase). The important implication from this model is that two *different* quinobenzoxazines or quinolones should be optimized for SAR rather than just a single molecule! In this way the two quinobenzoxazine (or quinolone) molecules interacting with DNA *and* the protein can each be independently fine-tuned for binding interactions.

Conclusions

The structure of a novel 4:4 quinobenzoxazine:Mg^{2+} complex assembled on DNA is proposed. In this complex the quinobenzoxazine−Mg^{2+} complex forms a "heterodimer" in respect to DNA in which one molecule is intercalated into DNA and the second molecule is bound externally, held to the first molecule by two Mg^{2+} bridges. The assembly of two such heterodimers forms a 4:4 complex in which the two externally bound molecules interact via π−π interactions (Figure 17, top). This proposed structure for a drug−DNA complex is a new paradigm for how drugs may interact with DNA and has structural features that mimic "leucine zippers", which dimerize on DNA through external hydrophobic interactions.[48]

Based upon cooperativity experiments with Norfloxacin, the structure of a mixed 4:4 quinobenzoxazine/Norfloxacin:Mg^{2+} complex is also proposed in which two Norfloxacin molecules replace the two externally bound quinobenzoxazines in the previous complex (Figure 17, bottom). The proposed structures (Figure 17) have important implications for the design of new topoisomerase II and bacterial gyrase inhibitors.

Experimental Section

Materials. Quinolone and quinobenzoxazine compounds were provided by Abbott Laboratories and used without further purification. Double-stranded calf thymus DNA, plasmid DNA pU19, poly[d(G-C)$_2$], and poly[d(A-T)$_2$] were purchased from Sigma. Synthetic oligodeoxynucleotides for the NMR experiments were purchased from Midland. Electrophoretic reagents (acrylamide, bisacrylamide, ammonium persulfate, and *N,N,N′,N′*-tetramethylethylenediamine) were purchased from BioRad. T4 polynucleotide kinase was from United States Biochemical Co., and DNase I was from Promega. The concentration of nucleic acids was determined spectrophotometrically. Molar absorptivities at 260 nm are reported as 6600 M^{-1} cm^{-1} for calf thymus DNA,[49] 7100 M^{-1} cm^{-1} for poly[d(G-C)$_2$], and 6600 M^{-1} cm^{-1} for poly[d(A-T)$_2$].[50]

DNA sequences of oligomers 1 and 2 used in the DNase I footprinting experiments are shown below:

Oligomer 1

5′-CGATCTTCGTCAAGCATCCCAGAAGGAAAAAATCGCCCTCGGACCAGGCAGCCTCAAACCCT-3′
3′-GCTAGAAGCAGTTCGTAGGGTCTTCCTTTTTTAGCGGGAGCCTGGTCCGTCGGAGTTTGGGA-5′

Oligomer 2

5′-GTCGCGTAAGTTGGCATTATAAAAAGCATTGCTTATCAATTTGTTGCAACGAACAGGTCACTGAATGCGCTGA-3′
3′-CAGCGCATTCAACCGTAATATTTTTCGTAACGAATAGTTAAACAACGTTGCTTGTCCAGTGACTTACGCGACT-5′

Agarose Gel Electrophoresis. Electrophoresis was carried out on a 2.5% agarose gel (10 × 8 × 0.5 cm) in TA buffer (0.04 M Tris-acetate), pH 8.0, at room temperature. Mixtures of A-62176 (1 μL, 10 mM) and salt stock solutions (1 μL, 0.5 M) were treated with a gel-loading buffer (0.5 μL) and electrophoresed at 100 V (~5.4 V/cm) for 1.5 h. The gels were photographed under UV light with a red filter.

Preparation of Oligomer DNA for DNase I Footprinting. The oligonucleotides (oligomers 1 and 2) used in this study were synthesized on an Applied Biosystems 381A DNA synthesizer using the phosphoramidite method. The crude oligomers were purified by preparative polyacrylamide gel electrophoresis. Purified oligomer was labeled with [γ-^{32}P]ATP using standard methods and annealed with the complementary strand to generate duplexes. Annealed duplexes were further purified using previously described methods.[27]

DNase I Footprinting. The 5′ ^{32}P-labeled oligomer DNA (5 ng) was mixed with a desired amount of A-62176 for 10 min at room temperature in 20 μL of a solution containing 10 mM Tris-HCl (pH 7.6), 10 mM NaCl, and 2 mM $MgCl_2$, unless otherwise indicated. Reaction mixtures were digested with 0.1 U of DNase I for 1 min. The DNase I reaction was stopped by the addition of 20 μL of sequence dye (80% formamide in 10 mM NaOH), and samples were loaded on a 10% denaturing sequence gel.

NMR Spectroscopy. All NMR spectra were recorded on a Bruker MSL-500 spectrometer at 27 °C. A-85226, an amino analog of A-62176, was chosen in the NMR study because it has greater solubility in water. ^{1}H-NMR experiments were carried out by adding aliquots of a concentrated drug solution to solutions of [d(G-C)$_5$]$_2$, [d(A$_4$GCT$_4$)]$_2$, and [d(A-T)$_5$]$_2$ in NMR buffer (10 mM NaH_2PO_4 and 100 mM NaCl, pH 7.0) in the presence of 100 mM $MgCl_2$ in 90% H_2O/10% D_2O. The total DNA concentration was 1 mM. ^{31}P-NMR experiments were carried out by adding A-85226 or ethidium bromide to [d(G-

$C)_5]_2$ solutions (1 mM) in NMR buffer in the presence of 100 mM $MgCl_2$ in D_2O. H_3PO_4 was used as an external reference (0.0 ppm).

FT-IR Spectroscopy. The FT-IR spectra were obtained with a Nicolet 550 IR spectrometer operating between 4000 and 400 cm^{-1} in KBr phase. Typically, 64 scans at a resolution of 4.0 cm^{-1} were averaged. The A-85226–Mg^{2+} complex was prepared by mixing A-85226 and excess $MgCl_2$ in H_2O and incubating at room temperature for 24 h. The mixture was then cooled in ice, and an orange suspension was obtained. The suspension was filtered, washed with ethanol, and dried in vacuum.

UV–Vis Spectrophotometric Titration. Absorbance spectra were recorded by a Perkin-Elmer 553 diode array UV–vis spectrophotometer. Aliquots (1–5 μL) of a 3 mM $MnCl_2$ solution containing drug at a concentration of 30 μM in MeOH were added to a 30 μM drug solution in MeOH. After addition of each aliquot, the absorption spectrum (290–500 nm) was recorded. Similar experiments were carried out for the drug–DNA interaction study. Sequential aliquots of a concentrated solution (5 mM base pair, ~1 μL) of nucleic acid containing drug at a concentration of 10 μM were added to a 10 μM drug solution containing 0.01 M Tris-HCl buffer with or without 10 mM $MgCl_2$ (pH 7.0) in a 1 cm cuvette. The total drug concentration was thus maintained at a constant value. After addition of each aliquot, the absorption spectrum (290–500 nm) was recorded. Addition of aliquots continued until either the absorbance became constant or the increasing concentration of nucleic acid itself caused a slight increase in absorbance.

Job Titrations. Separate stock solutions of metal ion and A-62176 at a concentration of 5 mM were prepared. A suitable amount of the metal ion and drug stock solutions was added to 1 mL of MeOH in a cuvette, resulting in 14 different [drug]/[Mn^{2+}] ratios between 0 and 1. The total concentration of (drug + Mn^{2+}) was kept constant at 100 μM. The absorbance (A) at 320 nm, which shows maximal change due to complex formation (Figure 4B), was measured. Subtraction of the absorbance (A_0) for the same drug concentration without Mn^{2+} from A yielded the absorbance change ($A - A_0$) due to complex formation. The $A - A_0$ values were normalized to the theoretical maximum absorbance change (A_{max}), which was obtained as described by Likussar and Boltz.[25] The normalized value, $y = (A - A_0)/A_{max}$, was then plotted against the mole fraction of drug (x_{drug}) to obtain the continuous variations plot or the Job plot.

Viscometric Titrations. Successive aliquots of 10 mM drug stock aqueous solution were added to a 5 mL sonicated calf thymus DNA (molecular weight ~ 2×10^5) solution (0.25 mM in 0.01 M Tris-HCl buffer, pH 7.0) in the reservoir of a Cannon-Ubbelohde semimicroviscometer (Cannon Instrument Co., series no. 50). The Mg^{2+} concentration was 25 mM. Under these conditions, the native double-helical structure of the DNA was not affected.[51] After each addition the flow time, t, was measured.

The specific viscosity was calculated by $\eta_{sp} = t/t_0 - 1$. Reduced viscosities (η_{sp}/C_N) were evaluated at one concentration only (for each value of ν), and intrinsic viscosities, [η], were calculated using a value of 0.53 for Huggins' coefficient k in eq 1:[52]

$$\eta_{sp}/C_N = [\eta](1 + k[\eta]C_N) \quad (1)$$

The concentration C_N refers to mol of nucleotide/L, irrespective of the amount of drug bound. Since the volume change was <1.5% during the titration, C_N was not corrected. Therefore, [η], which is the intrinsic viscosity for the drug–DNA complex, is calculated by substituting $\eta_{sp} = t/t_0 - 1$ into eq 1. The value of $[\eta]_0$ is the intrinsic viscosity for the DNA solution alone.

Cohen and Eisenberg[52] have shown that the ratios of the intrinsic viscosities depend upon the relative ratios of the contour length of DNA, L/L_0 (L and L_0 represent contour lengths in the presence and absence of drug) (eq 2).

$$L/L_0 \approx ([\eta]/[\eta]_0)^{1/3} \quad (2)$$

Equilibrium Dialysis. Since spectrophotometric titration is not sufficiently sensitive at low drug binding ratios (ν < 0.15), equilibrium dialysis was used to obtain binding data for this region. A 5 mL, 10 μM drug solution in a sealed dialysis tube (Spectro/Por, MWCO 6000–8000) as the first compartment was placed in a glass tube containing 8 mL of a calf thymus DNA (Sigma) solution at various concentrations (10 μM to 1 mM base pairs) as the second compartment. The whole assembly was placed in a shaker for 60 h at 20 °C in the dark. The calf thymus DNA used was predialyzed to eliminate short DNA strands. All solutions contained 5 mM $MgCl_2$ and were buffered by 20 mM phosphate at pH 7.0.

The intrinsic fluorescence of the drug was used to determine the free (C_f) and bound (C_b) drug concentrations. Fluorescence spectra were recorded on a Hitachi F-2000 fluorometer with an excitation wavelength at 380 nm. A-62176 has a weak fluorescence emission at ~500 nm in pH 7.0 buffer. Addition of DNA and Mg^{2+} increases the fluorescence intensity but produces very little spectral shift (data not shown). The fluorescence intensity (I) at 500 nm in the drug compartment was used to calculate drug concentrations (μM) in both compartments:

$$C_f = (I/I_0) \times 10 \quad (3)$$

$$C_b = [(5 \times 10) - (13 \times C_f)]/8 \quad (4)$$

where I_0 is the fluorescence intensity for 10 μM drug in the same buffer. The bound drug concentrations calculated in this way agree to within 5% with those calculated by fluorescence measurements of the solution outside the dialysis bag. The binding ratio (ν) can thus be calculated by

$$\nu = C_b/[DNA] \quad (5)$$

where DNA concentration is in base pairs.

Acknowledgment. This research was supported by grants from Abbott Laboratories, the Public Health Service (CA-49751), and the Welch Foundation. Jun-Yao Fan would like to acknowledge the financial assistance from IFUW in Switzerland. We thank Drs. Jacob Clement and Linus Shen (Abbott) for bringing these compounds to our attention and for ensuing useful discussions, Dr. Brad Chaires (University of Mississippi) for suggestions and help in analysis of the cooperativity experiments, Prof. Anthony Maxwell and his group (Leicester, U.K.) and Prof. Manlio Palumbo (Padua, Italy) for discussions on the proposed model, Mark Hansen for preparation of the molecular models, and David Bishop for preparing, proofreading, and editing the manuscript.

References

(1) Chu, D. T. W.; Maleczka, R. E., Jr. Synthesis of 4-Oxo-4*H*-quino-[2,3,4-*ij*][1,4]-benzoxazine-5-carboxylic Acid Derivatives. *J. Heterocycl. Chem.* **1987**, *24*, 453–456.
(2) Chu, D. T. W.; Hallas, R.; Clement, J. J.; Alder, L.; McDonald, E.; Plattner, J. J. Synthesis and Antitumor Activities of Quinolone Antineoplastic Agents. *Drugs Exp. Clin. Res.* **1992**, *18*, 275–282.
(3) Permana, P. A.; Snapka, R. M.; Shen, L. L.; Chu, D. T. W.; Clement, J. J.; Plattner, J. J. Quinobenzoxazines: A Class of Novel Antitumor Quinolones and Potent Mammalian DNA Topoisomerase II Catalytic Inhibitors. *Biochemistry* **1994**, *33*, 11333–11339.
(4) Sun, D.; Hurley, L. H.; Clement, J. J. Interaction of the Quinobenzoxazine Compound A-62176 with DNA. 84th Annual Meeting of the American Association for Cancer Research, Orlando, FL, 1993; Abstract No. 2063.
(5) Palumbo, M.; Gatto, B.; Zagotto, G.; Palù, G. On the Mechanism of Action of Quinolone Drugs. *Trends Microbiol.* **1993**, *1*, 232–235.

(6) Reece, R.; Maxwell, A. DNA Gyrase: Structure and Function. *Crit. Rev. Biochem. Mol. Biol.* **1991**, *26*, 335–375.
(7) Maxwell, A. The Molecular Basis of Quinolone Action. *J. Antimicrob. Chemother.* **1992**, *30*, 409–414.
(8) Mitscher, L. A.; Shen, L. L. A Cooperative Quinolone-DNA Binding Model for DNA Gyrase Inhibition. In *Nucleic Acid Targeted Drug Design*; Propst, C. L., Perun, T. J., Eds.; Marcel Dekker, Inc.: New York, 1992; pp 375–421.
(9) Gellert, M.; Mizuuchi, K.; O'Dea, M. H.; Nash, H. A. DNA Gyrase: An Enzyme That Introduces Superhelical Turns into DNA. *Proc. Natl. Acad. Sci. U.S.A.* **1976**, *73*, 3872–3876.
(10) Gellert, M.; Mizuuchi, K.; O'Dea, M. H.; Itoh, T.; Tomizawa, J.-I. Nalidixic Acid Resistance: A Second Genetic Character Involved in DNA Gyrase Activity. *Proc. Natl. Acad. Sci. U.S.A.* **1977**, *74*, 4772–4776.
(11) Sugino, A.; Peebles, C. L.; Kreuzer, K. N.; Cozzarelli, N. R. Mechanism of Action of Nalidixic Acid: Purification of *Escherichia coli* nalA Gene Product and Its Relationship to DNA Gyrase and a Novel Nicking-Closing Enzyme. *Proc. Natl. Acad. Sci. U.S.A.* **1977**, *74*, 4767–4771.
(12) Hooper, D. C.; Wolfson, J. S.; Souza, K. S.; Tung, C.; McHugh, G. L.; Swartz, M. N. Genetic and Biochemical Characterization of Norfloxacin Resistance in *Escherichia coli*. *Antimicrob. Agents Chemother.* **1986**, *29*, 639–644.
(13) Shen, L. L.; Pernet, A. G. Mechanism of Inhibition of DNA Gyrase by Analogues of Nalidixic Acid: The Target of the Drug Is DNA. *Proc. Natl. Acad. Sci. U.S.A.* **1985**, *82*, 307–311.
(14) Shen, L. L.; Baranowski, J.; Pernet, A. G. Mechanism of Inhibition of DNA Gyrase by Quinolone Antibacterials: Specificity and Cooperativity of Drug Binding to DNA. *Biochemistry* **1989**, *28*, 3879–3885.
(15) Shen, L. L.; Mitscher, L. A.; Sharma, P. N.; O'Donnell, T. J.; Chu, D. T. W.; Cooper, C. S.; Rosen, T.; Pernet, A. G. Mechanism of Inhibition of DNA Gyrase by Quinolone Antibacterials: A Cooperative Drug-DNA Binding Model. *Biochemistry* **1989**, *28*, 3886–3894.
(16) Shen, L. L.; Kohlbrenner, W. E.; Weigl, D.; Baranowski, J. Mechanism of Quinolone Inhibition of DNA Gyrase. *J. Biol. Chem.* **1989**, *264*, 2973–2978.
(17) Tornaletti, S.; Pedrini, A. M. Studies on the Interaction of 4-Quinolones with DNA by DNA Unwinding Experiments. *Biochim. Biophys. Acta* **1988**, *949*, 279–287.
(18) Palù, G.; Valisena, S.; Ciarrocchi, G.; Gatto, B.; Palumbo, M. Quinolone Binding to DNA Is Mediated by Magnesium Ions. *Proc. Natl. Acad. Sci. U.S.A.* **1992**, *89*, 9671–9675.
(19) Waring, M. J. Variation of Supercoils in Closed Circular DNA by Binding of Antibiotics and Drugs: Evidence for Molecular Models Involving Intercalation. *J. Mol. Biol.* **1970**, *54*, 247–279.
(20) Fan, J.-Y.; Sun, D.; Hurley, L. H. Structure of a Novel Intercalation Complex between the Antineoplastic Quinobenzoxazine, Magnesium Ion, and DNA: Implications for the Mechanism of Action of the Antibacterial Quinolones. 24th National Medicinal Chemistry Symposium, Salt Lake City, UT, 1994; Abstract No. 98.
(21) Sun, D.; Fan, J.-Y.; Kerwin, S.; Hurley, L. H. The Self-Assembly of a 4:4 Quinobenzoxazine to Mg^{2+} Partial Intercalation Complex on DNA: Implication for the Structure of the Quinolone Bacterial Gyrase-DNA Complex. The Fifth Conference on DNA Topoisomerase in Therapy, New York City, NY, 1994; Abstract No. 22.
(22) Behrens, N. B.; Mendoza-Diaz, G.; Goodgame, D. M. Metal Complexes of the Antibiotic Nalidixic Acid. *Inorg. Chim. Acta* **1986**, *125*, 21–26.
(23) Coppola, G. M.; Hardtmann, G. E. The Chemistry of 2*H*-3,1-Benzoxazine-2,4(1*H*)dione (Isatoic Anhydride). 7. Reactions with Anions of Active Methylenes to Form Quinolines. *J. Heterocycl. Chem.* **1979**, *16*, 1605–1610.
(24) Rao, C. N. R.; Randhawa, H. S.; Reddy, N. V. R.; Chakravorty, D. Vibrational Spectra of Alkali and Alkaline Earth Metal Complexes, Oxide Glasses, and Oxyanion Salts. *Spectrochim. Acta* **1975**, *31A*, 1283–1291.
(25) Likussar, W.; Boltz, D. F. Theory of Continuous Variation Plots and a New Method for Spectrophotometric Determination of Extraction and Formation Constants. *Anal. Chem.* **1971**, *43*, 1265–1272.
(26) Silva, D. J.; Kahne, D. Chromomycin A_3 as a Blueprint for Designed Metal Compounds. *J. Am. Chem. Soc.* **1994**, *116*, 2641–2642.
(27) Sun, D.; Hansen, M.; Clement, J. J.; Hurley, L. H. Structure of the Altromycin B (N7-Guanine)-DNA Adduct. A Proposed Prototype DNA Adduct Structure for the Pluramycin Antitumor Antibiotics. *Biochemistry* **1993**, *32*, 8068–8074.
(28) Feigon, J.; Denny, W. A.; Leupin, W.; Kearns, D. R. Interaction of Antitumor Drugs with Natural DNA: ^1H NMR Study of Binding Mode and Kinetics. *J. Med. Chem.* **1984**, *27*, 450–465.
(29) Kearns, D. R. High-Resolution Nuclear Magnetic Resonance Studies of Double Helical Polynucleotides. *Annu. Rev. Biophys. Bioeng.* **1977**, *6*, 477–523.
(30) Feigon, J.; Leupin, W.; Denny, W. A.; Kearns, D. R. Binding of Ethidium Derivatives to Natural DNA: A 300 MHz ^1H NMR Study. *Nucleic Acids Res.* **1982**, *10*, 749–762.
(31) Jones, R. L.; Wilson, W. D. Effect of Intercalating Ligands on the ^{31}P Chemical Shift of DNA. *J. Am. Chem. Soc.* **1980**, *102*, 7776–7778.
(32) Wilson, W. D.; Keel, R. A.; Mariam, Y. H. Effect of DNA Molecular Weight, Temperature, and Magnetic Field Strength on the ^{31}P NMR Results of DNA Complexes with Ethidium. *J. Am. Chem. Soc.* **1981**, *103*, 6267–6269.
(33) Wilson, W. D.; Jones, R. L. Interaction of Actinomycin D, Ethidium, Quinacrine, Daunorubin, and Tetralysine with DNA: ^{31}P NMR Chemical Shift and Relaxation Investigation. *Nucleic Acids Res.* **1982**, *10*, 1399–1410.
(34) Scatchard, G. The Attractions of Proteins for Small Molecules and Ions. *Ann. N. Y. Acad. Sci.* **1949**, *51*, 660–672.
(35) McGhee, J. D.; von Hippel, P. H. Theoretical Aspects of DNA-Protein Interactions: Co-operative and Non-Co-operative Binding of Large Ligands to a One-Dimensional Homogeneous Lattice. *J. Mol. Biol.* **1974**, *86*, 469–489.
(36) The observation that the DNase I footprinting and its viscometric titrations both show cooperativity but do not show the same extent of cooperativity is not unexpected. The DNase I footprinting experiments are measuring kinetics differences between the apparently more stable quinobenzoxazine dimers and the less stable mixed quinobenzoxazine–Norfloxacin dimers, while the viscometric titrations reveal a thermodynamic end point that is apparently different in the pure vs mixed dimers.
(37) Addess, K. J.; Gilbert, D. E.; Olsen, R. K.; Feigon, J. Proton NMR Studies of [*N*-MeCys^3,*N*-MeCys^7]TANDEM Binding to DNA Oligonucleotides: Sequence-Specific Binding at the TpA Site. *Biochemistry* **1992**, *31*, 339–350.
(38) Mendoza-Diaz, G.; Martinez-Aguilera, L. M. R.; Perez-Alonso, R.; Solans, X.; Moreno-Esparza, R. Synthesis and Characterization of Mixed Ligand Complexes of Copper with Nalidixic Acid and (N-N) Donors. Crystal Structure of [Cu(Phen)(Nal)-(H_2O)]-NO_3·3H_2O. *Inorg. Chim. Acta* **1987**, *138*, 41–47.
(39) However, on the basis of IR studies, these authors argue that the 4-keto group of nalidixic acid is not involved in complexes with Mg^{2+}. See: Mendoza-Diaz, G.; Pannell, K. H. Concerning the Coordination Site of the Antibiotic Nalidixate Ion towards Cu^{2+} Ions Using ^{13}C NMR. *Inorg. Chim. Acta* **1988**, *152*, 77–79.
(40) Cotton, F. A.; Wilkinson, G.; Gaus, P. L. *Basic Inorganic Chemistry*, 2nd ed.; John Wiley and Sons: New York, 1987.
(41) Ross, D. L.; Riley, C. M. Physicochemical Properties of the Fluoroquinolone Antibacterials V. Effect of Fluoroquinolone Structure and pH on the Complexation of Various Fluoroquinolones with Magnesium and Calcium Ions. *Int. J. Pharm.* **1993**, *93*, 121–129.
(42) Saenger, W. Left-Handed, Complementary Double Helices-A Heresy? The Z-DNA Family. *Principles of Nucleic Acid Structure*; Springer-Verlag: New York, 1984; p 283.
(43) Arnott, S.; Bond, P. J.; Chandrasekaran, R. Visualization of an Unwound DNA Duplex. *Nature* **1980**, *287*, 561–563.
(44) Rideout, D. Self-Assembling Cytotoxins. *Science* **1986**, *233*, 561–563.
(45) Gao, X.; Patel, D. J. Solution Structure of the Chromomycin-DNA Complex. *Biochemistry* **1989**, *28*, 751–762.
(46) Gao, X.; Patel, D. J. Antitumor Drug-DNA Interactions: NMR Studies of Echinomycin and Chromomycin Complex. *Q. Rev. Biophys.* **1989**, *22*, 93–138.
(47) Orphanides, G.; Maxwell, A. Evidence for a Conformational Change in the DNA Gyrase-DNA Complex from Hydroxyl Radical Footprinting. *Nucleic Acids Res.* **1994**, *22*, 1567–1575.
(48) Vinson, C. R.; Sigler, P. B.; McKnight, S. L. Scissors-Grip Model for DNA Recognition by a Family of Leucine Zipper Proteins. *Science* **1989**, *246*, 911–916.
(49) Mahler, H. R.; Kline, B.; Mehrotra, B. D. Some Observations on the Hypochromism of DNA. *J. Mol. Biol.* **1964**, *9*, 801–811.
(50) Wadkins, R. M.; Graves, D. E. Thermodynamics of the Interaction of m-AMSA with Nucleic Acids: Influence of Ionic Strength and DNA Base Composition. *Nucleic Acids Res.* **1989**, *17*, 9933–9946.
(51) Doty, P.; McGill, B. B.; Rice, S. A. Properties of Sonic Fragments of Deoxyribose Nucleic Acid (DNA). *Proc. Natl. Acad. Sci. U.S.A.* **1958**, *44*, 432–438.
(52) Cohen, G.; Eisenberg, H. Conformation Studies on the Sodium and Cesium Salts of Calf Thymus Deoxynucleic Acid (DNA). *Biopolymers* **1966**, *4*, 429–440.

JM940775G